Journal of Materials Chemistry B

ROYAL SOCIETY OF CHEMISTRY

REVIEW

View Article Online
View Journal | View Issue

Cite this: J. Mater. Chem. B, 2022, 10, 2761

Molybdenum disulfide (MoS_2)-based nanostructures for tissue engineering applications: prospects and challenges

Anuj Kumar, †*[ab] Ankur Sood†[a] and Sung Soo Han*[ab]

Molybdenum disulfide (MoS_2) nanostructures have recently earned substantial thoughts from the scientific communities owing to their unique physicochemical, optical and electrical properties. Although MoS_2 has been mostly highlighted for its industrial applications, its biological applicability has not been extensively explored. The introduction of nanotechnology in the field of tissue engineering has significantly contributed to human welfare by displaying advancement in tissue regeneration. Assimilation of MoS_2 nanostructures into the polymer matrix has been considered a persuasive material of choice for futuristic tissue engineering applications. The current review provides a general discussion on the structural properties of different MoS_2 nanostructures. Further, this article focuses on the interactions of MoS_2 with biological systems in terms of its cellular toxicity, and biocompatibility along with its capability for cell proliferation, adhesion, and immunomodulation. The article continues to confer the utility of MoS_2 nanostructure-based scaffolds for various tissue engineering applications. The article also highlights some emerging prospects and possibilities of the applicability of MoS_2-based nanostructures in large organ tissue engineering. Finally, the article concludes with a brief annotation on the challenges and limitations that need to be overcome in order to make plentiful use of this wonderful material for tissue engineering applications.

Received 17th January 2022,
Accepted 20th February 2022

DOI: 10.1039/d2tb00131d

rsc.li/materials-b

1. Introduction

The development of novel materials has widened the scope of their utility in numerous commercial applications. With the evolution of nanotechnology, the use of orthodox materials and production methods have been sidetracked and superseded with new methodologies, and novel engineered materials with remarkable features. It would not be an embellishment to exclaim this era as the epoch of nanomaterials. Nanomaterials offer distinctive properties compared to their counter bulk part, which makes them a unique and interesting class of materials.[1]

On a broader prospect, nanomaterials are classified as zero-(0D), one-(1D), two-(2D), and three-dimensional (3D) based on their shapes and structures.[2] Until recently, 2D nanostructures and layered materials have marched rapidly and have lured the attention of many researchers around the world, as an elegant and efficient class of nanomaterials in a wide range of applications such as energy storage,[3] transparent electrodes,[4] wearable devices,[5] cancer treatment,[6] and biosensing.[7] Since the inception of graphene in 2004, the first known 2D material, remarkable progress has been perceived on atomically thin 2D materials with diverse applications across various scientific turfs.[8] Features like transparency, high electrical and thermal conductivity, high specific surface area and young's modulus have marked the success of this fascinating class of material.[9] Owing to these stupendous properties along with the shortcoming of zero band gap, efforts have been bestowed to further explore 2D graphene analogues with semiconducting nature. In this regard, Transition Metal Dichalcogenides (TMD) with the general representation of MX_2 (M as a transition metal atom (Mo, W, Ta, *etc.*)) and X is a chalcogen atom (S, Se, Te, *etc.*) have emerged as promising alternatives.[10] Within a single layer of TMD, X–M–X atoms are bonded covalently in a hexagonally packed plane and such single layers are bound together by weak van der Waals forces. The TMD monolayer crystal offers distinctive properties compared to their bulk analogues due to the lack of a center of inversion, which allows admittance to a new degree of freedom, the k-valley index, and led to a new field of physics called valleytronics.[11,12]

TMD demonstrates a distinctive amalgamation of the direct band gap, resilient spin–orbital coupling, atomic-scale thickness, high conductivity along with promising electronic and mechanical properties. These features inscribe its attainment

[a] School of Chemical Engineering, Yeungnam University, 280 Daehak-ro, Gyeongsan 38541, Korea. E-mail: anuj.budhera@gmail.com, sshan@yu.ac.kr
[b] Institute of Cell Culture, Yeungnam University, 280 Daehak-ro, Gyeongsan 38541, Korea
† Equal contribution.

as a proficient material for applications in high-end electronics, energy harvesting, flexible and wearable electronics, DNA sequencing and personalized medicine.[13] Among different layered TMDs, molybdenum disulfide (MoS_2) has gained tremendous attention owing to its fascinating properties such as ease of synthesis, high catalytic properties, exceptional on/off ratio, satisfactory biocompatibility, and enormous direct band gap of 1.8 eV for the monolayer.[14,15]

MoS_2 has achieved prime progress in the field of optoelectronics,[4,16] energy storage[17] and conversion,[18] hydrogen evolution reaction (HER),[19,20] and next-generation switches.[21,22] Moreover, MoS_2 layers are often associated with crystal-dependent fluorescence[23] or the ability to quench fluorescence.[24] In addition, thin nanosheets of MoS_2 exhibit strong absorbance in the near-infrared region (NIR)[25] along with efficiency for photothermal conversion.[26] Also, the constituents of MoS_2, *i.e.* molybdenum, and sulfur also play a key role in maintaining biological systems.[27] All these characteristics along with the key attribute of MoS_2 of having very high specific surface area makes imperative utilization of this fascinating material across diverse biomedical applications, which include but are not limited to drug delivery,[28,29] antibacterial activity,[30–32] biosensing,[33,34] and theranostics.[35,36]

Humans have always envisaged the revamping of damaged organs and tissues with passable functioning, an aspiration, which is feasible using tissue engineering. In tissue engineering, cells/tissues, scaffolds, reinforcements, and growth factors are coalesced to invigorate or amend damaged or pathologically alimented tissues.[37] Lately, a wide range of 2D nanostructures has been explored for their utility for tissue engineering applications.[38] A comprehensive review by Liu *et al.* although focuses on the use of MoS_2-based nanostructures for biomedical applications[27] it has not highlighted its use in tissue engineering applications. Another review by Yadav *et al.* describes the application of 2D MoS_2-based nanostructures specifically for biosensing,

Anuj Kumar

Dr Anuj Kumar is an Assistant Professor (International Faculty Member)-Polymers & Biomaterials in the School of Chemical Engineering at the Yeungnam University (YU), South Korea. During this tenure, he has been awarded three sponsored research projects (two NRF projects as Principal Investigator (PI) and one Indo-Korea joint research project awarded jointly by MSIT-NRF Korea/DST India as Co-PI) for developing injectable and 3D printable hydrogels for soft and hard tissue regeneration. Prior to this position, he was Postdoctoral Research Associate in YU and Assistant Professor (Chemsitry) in DIT University, Dehradun (India). He received his PhD (Polymer Science and Engineering), MTech (Fibre Science and Technology), and MSc (Organic Chemistry) from Indian Institute of Technology Roorkee (IITR), Indian Institute of Technology Delhi (IITD), and Chaudhary Charan Singh University Meerut (CCSUM), India, respectively. He has authored more than 60 publications in internationally reputed journals, 1 book, and 10 book chapters. His research interests are focused on sustainable biomass, nanocellulose, biopolymers, hydrogels, design of biomaterials/nanobiomaterials, 3D bioprinting, microfluidics, tissue engineering, drug delivery systems, cancer therapy, wearable bioelectronics, etc.

Ankur Sood

Dr Ankur Sood received his PhD in the field of drug delivery and imaging applications of nanoparticles from GGS Indraprastha University, New Delhi, India. He worked as a Research Associate at the Institute of Nano Science and Technology, Punjab, India. During this tenure he worked on polymer/metal nanocomposites and fluorescent gold clusters for biomedical applications. He worked as Senior Project Scientist at Indian Institute of Technology; Mandi, India where his work was focused on polymer nanoparticles based drug delivery systems. He was Postdoctoral Research Fellow in Yeungnam University, South Korea till February 2022 and currently he is working as an Assistant Professor (International Faculty Member) in School of Chemical Engineering at the Yeungnam University, South Korea. His current research is focused on 3D bioprinting, tissue engineering, and inorganic/organic nanoparticles for drug delivery and biosensing applications.

Sung Soo Han

Dr Sung Soo Han is a Professor at the School of Chemical Engineering, Yeungnam University (YU), South Korea. He received his PhD, MS, and BS degrees from the Department of Polymer and Textile Engineeirng, Seoul National University (SNU), Seoul, South Korea. He has been awarded various NRF funded projects including one Indo-Korea joint research project awarded jointly by MSIT-NRF Korea/DST India as PI). He has published many research and review articles in internationally reputed journals. His research interests are focused on biomaterials, nanomaterials, tissue engineering, drug delivery, cancer therapy, bioprocess engineering, and artificial meat culture.

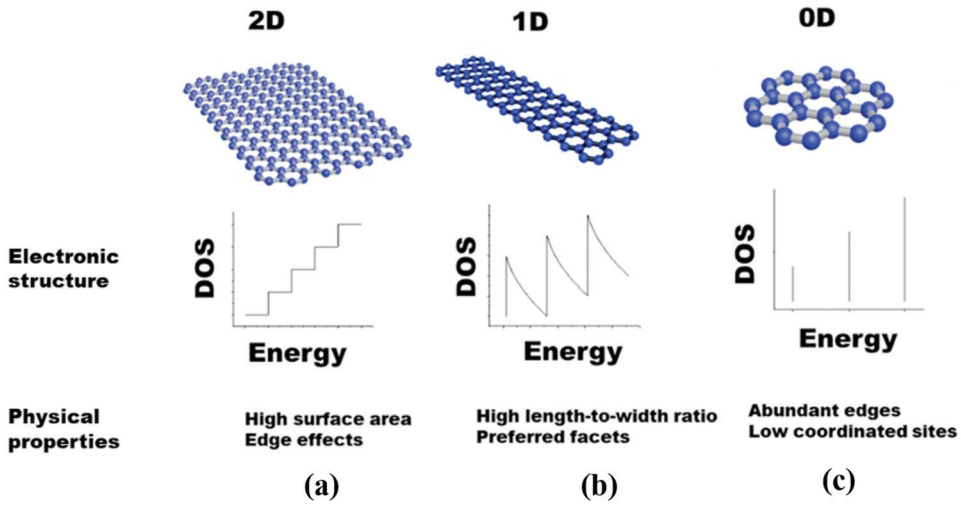

Fig. 1 Classification, electronic structure, and physical properties of (a) two-dimensional (2-D), (b) two-dimensional (1-D), and (c) zero-dimensional (0-D) materials. (DOS: Density of States). Reproduced with permission from.[64] Copyright 2020 Elsevier.

bioimaging and therapeutics.[2] Moreover, the review of Nguyen *et al.* mainly focuses on the surface properties of 2D materials from biosensing to tissue engineering.[39] However, to date, no dedicated review is published on the application of MoS_2 nanostructures in tissue engineering applications. In the current review, we aim to explore the three main structural morphologies of MoS_2, *i.e.* nanosheets, nanotubes, and quantum dots with their inherent properties. The review also focuses on the interaction of MoS_2 nanostructures with biological systems. With this review, a spotlight is also shed on the utility of MoS_2-based scaffolds for various tissue engineering applications. Finally, the review highlights some key shortcomings in using MoS_2-based materials for tissue engineering applications that could be addressed to make this potential material a significant performer for next-generation tissue engineering applications.

2. Structure and properties of different forms of MoS_2 nanostructures

The diverse electronic properties of TMDs result from the filling of the non-bonding d bands from group 4 to group 10 species.[40] TMDs exhibit metallic properties, when the orbitals are partially occupied, whereas when the orbitals are fully occupied, TMDs display semiconducting properties. On the contrary, compared to the influence of metal atoms, chalcogen atoms exhibit a minor impact on the electronic structure; however, it is examined that upon broadening of the d bands, the band gap decreases by increasing the atomic number of the chalcogen.[41]

MoS_2 has a 2D layered structure with each layer of thickness of about 0.65 nm, which are heaped upon each other to form bulk. Weak van der Waals forces clasp these layers together.[42] MoS_2 exists in three different crystal structures namely, a trigonal phase (1T), a hexagonal phase (2H), and a rhombohedral phase (3R). The letters in the representation correspond to the crystal structures whereas the digits represent the number of monolayers in the unit cell. The Mo–S coordination is octahedral in the IT phase, while the coordination is trigonal prismatic in the case of 2H and 3R phases, respectively.[43] Naturally existing MoS_2 crystals (*e.g.* molybdenite) mostly occur in the 2H phase, which is also the thermodynamically stable phase, while synthetic MoS_2 mainly comprises 1T and 3R phases and are metastable in nature.[44] The next section describes different forms of MoS_2 nanostructures.

2.1. 2D MoS_2 (nanosheets)

With the great success of graphene, researchers are motivated with an equivalent encouraging surge to develop alternate 2D materials that could result in the formation of atomic sheets with astonishing properties.[45,46] Among all known 2D TMDs, MoS_2 is one such material that is accompanied by a naturally layered structure, which makes it convenient to fabricate eminent quality 2D nanosheets without making much efforts during the synthesis process[47,48] (Fig. 1(a)). The conversion process of MoS_2 from bulk to single-layered nanosheets imparts direct bandgap, resulting in exceptional photoelectric properties.[49] This significant bandgap transition is accompanied by strong fluorescence emission signals in the visible reason, which could be explored for numerous cost-effective biomedical applications such as biosensing and imaging.[50] Owing to the large lateral dimensions, MoS_2 nanosheets are easily dispersible in liquid/gaseous media. In addition, by engineering the edges of MoS_2 nanosheets, to be terminated with either Mo or S atoms, the overall electrical performance of the nanosheets could be fine-tuned. These properties serve as vital prerequisites for many applications involving electrochemical biosensors.[51] Many researchers have elucidated the unique properties of MoS2 nanosheets. Castellanos-Gomez *et al.* assessed the elastic properties of a suspended portion of MoS_2 nanosheets (5–25 layered) using AFM and reported an exceptionally high Young's modulus (E = 0.33 ± 0.07 TPa) for the nanosheets.[52] Further, the stiffness and breaking strength

of ultrathin MoS_2 nanosheets were measured and reported by Bertolazzi *et al.*[53] The enhancement in mechanical properties of 2D MoS_2 could be explored as a reinforcement material for numerous tissue-engineering applications, especially for bone tissue engineering. Even though MoS_2 nanosheets display a range of novel properties that are remarkably discrete from their bulk counterparts, the production of large-scale and defect-free atomic layers of MoS_2 with desired thickness and control over substrates is still a challenging task.

2.2. 1D MoS_2 (nanotubes)

2D TMD materials have gained considerable attention from the scientific community owing to their remarkable properties compared to their bulk analogues.[54] Over the past decade, much of the research revolved around MoS_2-based nanostructures, a key ambassador of the TMD family. As the dimension of MoS_2-based nanostructures is reduced to a single or few layers, these materials tend to sustain their semiconducting nature and thereby uncover extraordinary physicochemical properties.[55] Further modification in the structure of 2D TMDs is achieved by draping individual layers, resulting in the formation of chiral cylindrical-like structures known as 1D nanotubes[56] (Fig. 1(b)).

1D nanomaterials embrace two out of the three dimensions in the nano regime, while the third dimension is in the micrometer range.[57] In the year 2000, Seifert *et al.* proposed the existence of MoS_2 nanotubes in mainly two forms, zigzag and armchair.[58] They reported a narrow direct band gap associated with zigzag MoS_2 nanotubes, while the armchair MoS_2 nanotubes demonstrate a nonzero moderate direct gap. Moreover, the alteration in their structural arrangement has direct implications on their electrical properties.[59] The cylindrical tube-like arrangement of MoS_2 nanotubes serves as containers in which molecules/nanomaterials could be trapped. These properties could further be explored for numerous biomedical applications including biosensing, bioimaging and drug delivery.[60,61] The bond length of MoS_2 nanotubes is slightly more than MoS_2 nanosheets. Further, MoS_2 nanotubes share a similar band structure with carbon nanotubes with the exception that in the case of MoS_2 nanotubes the bandgap augments as the diameter of the nanotubes increases.[62] Efforts are being made to fabricate hybrids MoS_2 nanotubes, which could offer the property of high mechanical strength that is a key requirement of bone tissue engineering. Also designing hollow tubes could be of high importance for nerve tissue engineering. MoS_2 nanotubes could also be used as reinforcement for polymer scaffolds in order to improve their thermal and mechanical strength. Several key issues must be addressed if 1D MoS_2 nanotubes are to be realized for their complete scientific and technological potential in the field of tissue engineering.

2.3. 0D MoS_2 (quantum dots)

The size of quantum dots (QDs) is in the range of 2–10 nm. At these low dimensions, the quantity of atoms existing in the material reduces. This reduction in the number of atoms results in a significant drop in the number of overlapping energy levels, thereby increasing the energy gap between the valence band and the conduction band. The energy levels of the electrons in this state are not continuous but tend to form a discrete set of energy bands, a phenomenon known as quantum confinement. Due to quantum confinement and edge effect, the QDs present remarkable optical, and chemical properties[63] (Fig. 1(c)).

Monolayer MoS_2 QDs have become an important class of materials due to their outstanding properties that include abundant active edge sites, high specific surface area, exceptional electrical conductivity and photophysical properties along with strong hydrogen adsorption properties.[65,66] These characteristics make it a potent material for applications such as electrocatalysts for hydrogen evolution reactions (HERs), and energy storage.[67] MoS_2 QDs comprise monolayered hollow closed nanostructures, with the smallest permitted unit ''nanooctahedra'' within the range of 3–8 nm[33] and can be classified as n-type semiconductors as determined by Vikraman *et al.* by fabricating field-effect transistors (FETs) utilizing thin MoS_2 QD layers.[68] A decrease in the size of bulk material in the nano regime within the range of QDs tends to impart strong optical nonlinearity properties making QDs a favourable photoluminescence material.

The impact of size variation in MoS_2 QDs is linked to their optical properties, which in turn can be tweaked by altering the size of MoS_2 QDs. As the confinement energy is dependent on the size of the QD, the emission wavelength is precisely linked to the QD size. With the alteration in the size of QDs, the band gap changes, these results in altered emission and absorption of light. For a QD with less confinement, the size is bigger thereby reflecting color towards the reddish side, and the more the confinement, the lesser is the size of QDs, the bluish it is. The optical properties of MoS_2 QDs also cover their ability for photoluminescence, which is significantly dependent on the excitation wavelength. It is well acknowledged in the literature that polydispersed MoS_2 QDs exhibits significantly more excitation-dependent emission compared to monodispersed MoS_2 QDs.[69] This notion is remarkably dependent on the adsorption of oxygen atoms at the edges of QDs thus creating defects.[70] The optical properties of MoS_2 QDs are of significant importance in terms of biomedical applications such as real-time imaging,[71] biosensing,[72] drug delivery,[73] and early cancer diagnosis.[18] Even though MoS_2 QDs are at a very early stage in the field of tissue engineering, the remarkable properties of this material have opened a new arena for innovative aspects in tissue engineering and regenerative medicines. Table 1 summarizes the different fabricating strategies for different MoS_2 nanostructures.

3. Cellular interactions of different forms MoS_2 nanostructures

3.1. Biocompatibility and cellular toxicity

In order to fabricate a material with its utility for biological interactions, biocompatibility and cytotoxicity assessment play a crucial role. It is a well-documented notion that cell penetration

Table 1 Fabrication strategies of different MoS_2 morphology

S. no	Morphology	Processing method	Exfoliating agent/solvent/substrate	Features	Ref.
1.	Nanosheets	Solvothermal method	Heptamolybdate tetrahydrate, thiourea (NH_2CSNH_2), oleylamine	Enhanced biological properties and cellular response	74
2.	Nanosheets	Supercritical hydrothermal process	Molybdenum trioxide (MoO_3), ascorbic acid (AA), formic acid (FA)	MoS_2 sheets with 6–7 layers, precise control over the phase and number of layers of MoS2, very fast process	75
3.	Nanosheets	Chemical vapour deposition (CVD)	MoO_3, sulphur (S) powder	Large surface area (1 cm^2), vertically aligned, thickness of $\leq$50 nm	76
4.	Nanosheets	Probe sonication method	Bulk MoS_2, poly (acrylic acid)	High yield of approximately 100%, nanosheets with 5–6 layers, peroxidase mimicking activity	77
5.	Nanosheets	Microwave-assisted hydrothermal synthesis	Sodium molybdate dehydrate, NH_2CSNH_2, cellulose paper	Responsivity of 290 mA W^{-1}, Detection up to 1.8 $\times$ 10^9 Jones, external quantum efficiency of 37%	78
6.	Nanosheets	Heating-up approach	1-Dodecanethiol	Thickness of approximately 100 nm, offers electrical bistability and NDR behaviour	79
7.	Nanosheets	Ultrasonication and chemical route	Sodium molybdate hexahydrate, NH_2CSNH_2, polydopamine, carbon nanotubes	Reversible capacity of 747.3 mA h g^{-1} and 512.4 mA h g^{-1} over 200 cycles at 200 mA g^{-1} for sodium-ion batteries (SIB) and lithium-ion batteries (LIB) after 100 cycles	80
8.	Nanosheets	Hydrothermal method	MoO_3, L-cysteine	Reversible capacity of 1097 mA h g^{-1} at a current density of 50 mA g^{-1} after 25 cycles for LIB	81
9.	Nanosheets	CVD	SiO_2/Si substrate, MoO_3, S element	Uniform grain size reaching upto 146 μm, precise control over intermediate product (MoO_{3-x})	82
10.	Nanosheets	Solid-state reaction method		The figure of merit $\sim$2.52 $\times$ 10^{-15} esu cm, optical limiting (OL) effects with low threshold F_{OL} $\sim$ 44 mJ cm^{-2}	83
11.	Nanotubes	Catalyst-free vapour–gas–solid reaction	$H_8N_2MoS_4$, nitric acid, sodium dodecyly sulphate	Diameter 30–200 nm, multiwall structure	84
12.	Nanotubes	Hydrothermal method	$(NH_4)_6Mo_7O_{24}{\cdot}4H_2O$, ethylenediamine (EDA), L-cysteine	Hollow tubes, rate cyclability (127 mA h g^{-1} at 200 mA g^{-1} after 100 cycles in the potassium ion battery)	85
13.	Nanotubes	Gas–solid reaction	$H_8N_2MoS_4$	Open ended tubes, outer diameter $\sim$25 nm, inner diameter is $\sim$12 nm	86
14.	Nanotubes	Hydrothermal method	$H_8N_2MoS_4$, EDA, hydrochloric acid	Reversible capacity of 1327 mA h g^{-1} at 0.1 C and 850 mA h g^{-1} at 5 C after 300 cycles for LIH, reversible capacity of 480 mA h g^{-1} at 0.5 C after 200 cycles for SIB	87
15.	Quantum dots	Colloidal chemical route	$H_8N_2MoS_4$, oleyl amine	Quantum yield of 4.4%, thickness of approximately 3 nm	69
16.	Quantum dots	Hydrothermal method	$H_8N_2MoS_4$	Blue fluorescent MoS_2 QDs, narrow lateral size distribution, detection of hyaluronidase	72
17.	Quantum dots	Laser ablation	Bulk MoS_2	Fast, green, and one-step process to synthesize MoS_2 QDs, High electrocatalytic activity for hydrogen evolution reactions (HERs), high yield of 36.73 wt%,	65
18.	Quantum dots	Liquid nitrogen quenching & chemical routes	Bulk MoS_2, isopropanol	Narrow lateral size distribution (1.41 nm), quantum yield of 5.06%	88
19.	Quantum dots	Pulsed Laser ablation	Bulk MoS_2	Average size 2–8.5 nm, high electrocatalytic activity for HERs, high aqueous dispersion stability	89
20.	Quantum dots	Electrochemical method	Lithium bis-trifluoromethylsulphonylimide, n-type porous silicon (PS)	Significant improvement in electroluminescence performance, enhancement in F band	90
21.	Quantum dots	Wet grinding and co-solvent sonication	Bulk MoS_2, *N*-methyl-2-pyrrolidone, 1,2-dichlorobenzene	Quantum yield of 7 mg mL^{-1}, average size range of 2–5 nm, blue luminescence upon UV excitation	91
22.	Quantum dots	CVD	MoO_3, S powder	Single layered 2H–MoS_2 structure, diameter of 4–7 nm, Density of 10^{11} cm^{-2}	92
23.	Quantum dots	Hydrothermal method	$H_8N_2MoS_4$	Sensing of adenosine triphosphate, linearity for 0–200 μM for Fe^{3+} and 0–140 μM for ATP	93
24.	Quantum dots Miscellaneous	Laser ablation method	Bulk MoS_2, *n*-hexane, *n*-butyllithium	Diameter of 10 nm, retention time of 10 s	94

Table 1 (*continued*)

S. no	Morphology	Processing method	Exfoliating agent/solvent/substrate	Features	Ref.
1.	Thin films	Polymer-assisted deposition, thermolysis	Anhydrous ammonium tetrathiomolybdate ($(H_8N_2MoS_4)$ linear-poly(ethylenimine)	Uniform thickness (6 in), fast photoresponse (<1 ms), High on–off ratio (~10^4)	95
2.	Edge terminating films	Sulfurization/selenization process	SiO_2/Si	Vertically aligned layers, HER catalysis,	96
3.	Single-crystal	Hybrid thermolysis	p-Si wafer	High-quality p–n heterojunctions, generation of highly crystalline product	97
4.	Films	Chemical Vapour Deposition (CVD)	Amorphous SiO_2 substrate	Highly crystalline, large area atomic layers	98
5.	Metallic films	Laser irradiation at low temperature	Polyethylene terephthalate (PET)	Fast response, controllable shape, ability for patterning	99

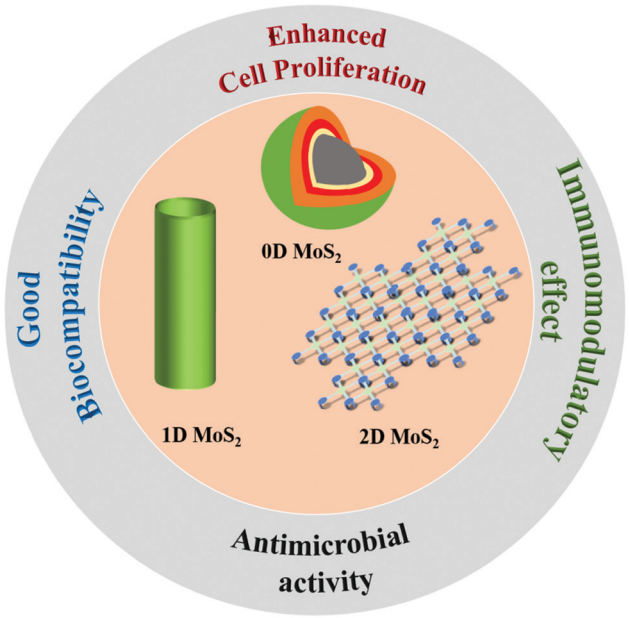

Fig. 2 Features of MoS_2-based nanostructures for cellular interactions.

and cleavage of active cell lines are the two main hurdles that restrict the clinical use of any nanomaterials.[100,101] Recently, MoS_2 nanostructures have been widely explored for their biological interactions with cell membranes due to the large surface area.[102] The unique features of MoS_2 nanostructures have supported its utility as a potent material for numerous biomedical applications[103–105] (Fig. 2). Despite the reported compatibility of MoS_2 nanostructures for biomedical applications, MoS_2 nanomaterials have also been associated with the provocation of cellular membrane damage in different unicellular systems.

In this regard, Chng *et al.* studied the dependency of the level of toxicity on the extent of exfoliation of MoS_2. This work demonstrated that the lesser exfoliated MoS_2 presents more level of toxicity.[106] Through this work, the severity of the mechanical interaction between the cellular membrane and MoS_2 nanostructures was assessed, which is accounted for the phospholipids extraction, which in turn destroys the integrity of the membrane, directing to cytoplasm leakage and finally cell death. Analogous work was also highlighted by Wu *et al.* in the case of *E. coli* and *S. aureus*. The study revealed the interactions between MoS_2 nanosheets and membrane phospholipids supported by experimental and simulation-based data.[107] The interaction of materials with the biological system has to undergo a series of events starting from adhesion followed by recognition and finally internalization. The first encounter of any material with the cell membrane decides its fate and journey. The studies highlighted above are concerned to access the toxicity of MoS_2 nanosheets and their interaction with the phospholipids present in the cellular membrane. The results will have a significant impact on the utility of MoS_2 nanostructures while designing scaffolds for tissue engineering applications.

Given the above context, investigation concerning biocompatibility assessment of MoS_2 nanostructures is an essential

matter. In this regard, Yang *et al.* reported the linkage of the antibacterial activity of chemically exfoliated 2D MoS_2 nanosheets to the production of reactive oxygen species (ROS).[108] Further, Shun *et al.* reported the enhancement in the antibacterial properties and cellular response upon modification of MoS_2 with ultrafine-grained titanium.[109] Along this line, Fan *et al.* demonstrated the capability of single-layered MoS_2 nanosheet suspensions to offer photocatalytic antimicrobial activity upon exposure to visible light under the influence of an electron donor, ethylenediaminetetraacetic acid (EDTA).[110] In this case, the EDTA is responsible for transferring electrons to MoS_2, which results in increased light absorption and augmented the separation of photoelectron–hole pairs, which enhances the ROS yield, resulting in high antibacterial performance. Moreover, few studies have also reported enhancement of the photothermal performance of MoS_2 under light irradiation,[111] and ROS-independent oxidative stress, disturbing bacterial structure and vital functions[112] as the reason for the antibacterial property of MoS_2 based nanostructures.

The ability to impart antimicrobial properties makes MoS_2 nanostructures a compelling candidate for wound healing and tissue engineering applications. Moreover, the work carried out by Teo *et al.* demonstrated the fact that TMDs are less toxic compared to their graphene analogues.[113] The study also emphasized the non-suitability of MTT assay as the sole criteria to assess the cytotoxicity evaluation of nanomaterials.

The pulmonary hazard of 2D MoS_2 compared to the aggregated MoS_2 (Agg-MoS_2) was studied by Wang *et al.* The data obtained from this study suggested the attenuation of toxicity levels under exfoliation for 2D MoS_2 compared to Agg-MoS_2.[114] This data provide an important understanding towards the safety assessment of 2D MoS_2 for biomedical applications. Further, Domi *et al.* studied the fate of commercially available colloidal solutions of MoS_2 and studied their physicochemical and toxicological responses at *in vitro* levels.[115] The study emphasized the importance of the biocompatibility of the MoS_2 nanoparticles as a key factor affecting cellular interactions.

Further, the degradation of MoS_2-based nanostructures could also present vital stats in terms of applications in biological systems. In this context, Wang *et al.* carried out a detailed study on the degradation pathway in biologically relevant media and presented a detailed analysis emphasizing the molecular oxygen-driven dissolution process of MoS_2 nanosheets in biological media.[116] It is well documented that MoS_2 can be decomposed when exposed to hydrogen peroxide (H_2O_2) due to the change in the oxidation state from Mo(IV) to Mo(VI), mostly in the form of MoO_3/MoO_4^{2-} ions while releasing sulphur, which plays a central role in many biological activities and functions (*e.g.*, a constituent of sulfur-containing amino acids, formation and activity of iron–sulfur proteins, *etc.*).[117–119] Moreover, Kurapati *et al.* studied the degradation of MoS_2 nanosheets at a physiological concentration of H_2O_2.[120] In this study, the biodegradation of MoS_2 materials has also been examined using enzyme models of peroxidase enzyme horseradish peroxidase (HRP), and human myeloperoxidase (MPO) under the exposure of low concentration of H_2O_2. An elementary understanding of the degradation mechanisms, followed pathway, and the performance of the resulting by-products of MoS2 nanostructures in biofluids is very crucial to further maximize the potential benefit that could be extracted from them for their application in the field of tissue engineering. In addition, the biodistribution and clearance behaviour of nanomaterials are vital for their utility in biomedicines/nanomedicines. To understand the clearance of PEGylated-MoS_2, Hao *et al.* carried out a study, which depicted the accumulation of PEGylated MoS_2 nanostructures mostly in reticuloendothelial systems (RES) organs such as liver and spleen both at *in vitro* and *in vivo* levels.

Although, the data for cytotoxicity evaluation of MoS_2 nanostructures are minimal, the assessment of their biocompatibility along with stability and degradation upon interaction with the biological system could provide insights into the impact of MoS_2 in the field of biomedical sciences. Understanding the interaction of MoS_2 nanostructures at the cellular level could be of high importance to develop MoS_2 reinforced scaffolds for tissue engineering applications.

3.2. Cellular adhesion and proliferation

2D nanomaterials have been receiving incessant consideration from the scientific communities due to their remarkable features of chemical functionality and structural anisotropy.[121] Recently, MoS_2 nanostructures have been extensively investigated for numerous applications due to their band gap tenability.[122] Recently, these properties are being explored for photothermal therapies[123,124] and applications concerning cellular interactions.[125,126] In terms of cellular interaction, cell adhesion and proliferation plays a crucial role in getting adequate cellular responses. Understanding the mechanistic pathway concerning cell proliferation upon interaction with MoS_2 could lead to different application-oriented strategies. A lot of new outcomes could be uncovered concerning photo-based therapies, early diagnosis, cancer treatment and especially tissue engineering applications, where the fate of the treatment process heavily depends on the cellular response, interaction, and proliferation. In this regard, Ke *et al.* fabricated a gold nanoparticles-modified monolayer MoS_2 sensor, capable of rapidly detecting DNA molecules with high sensitivity, and selectivity.[127] The study was based on the change in the dielectric environment of the MoS_2-based probe upon the interaction with nucleosides of DNA, which in turn alters the band gap of MoS_2. The sensitivity of this probe in real-time applications will certainly depend on the interaction of cells with the MoS_2-based probe system. This work may have applicability while designing scaffolds for tissue engineering applications with real-time monitoring.

Further, Carrow *et al.* studied the interaction of 2D MoS_2 and human mesenchymal stem cells (hMSCs) at the molecular level.[128] Here, the synthesized exfoliate 2D MoS_2 nanosheets were physicochemically evaluated using XRD, AFM, TEM, Raman spectroscopy and XPS. Further, it was reported that the photoluminescent intensity for exfoliated MoS_2 decreased upon lithium (Li) intercalation; subsequently, the phase transition from semiconducting 2H to metallic 1T phase took place.

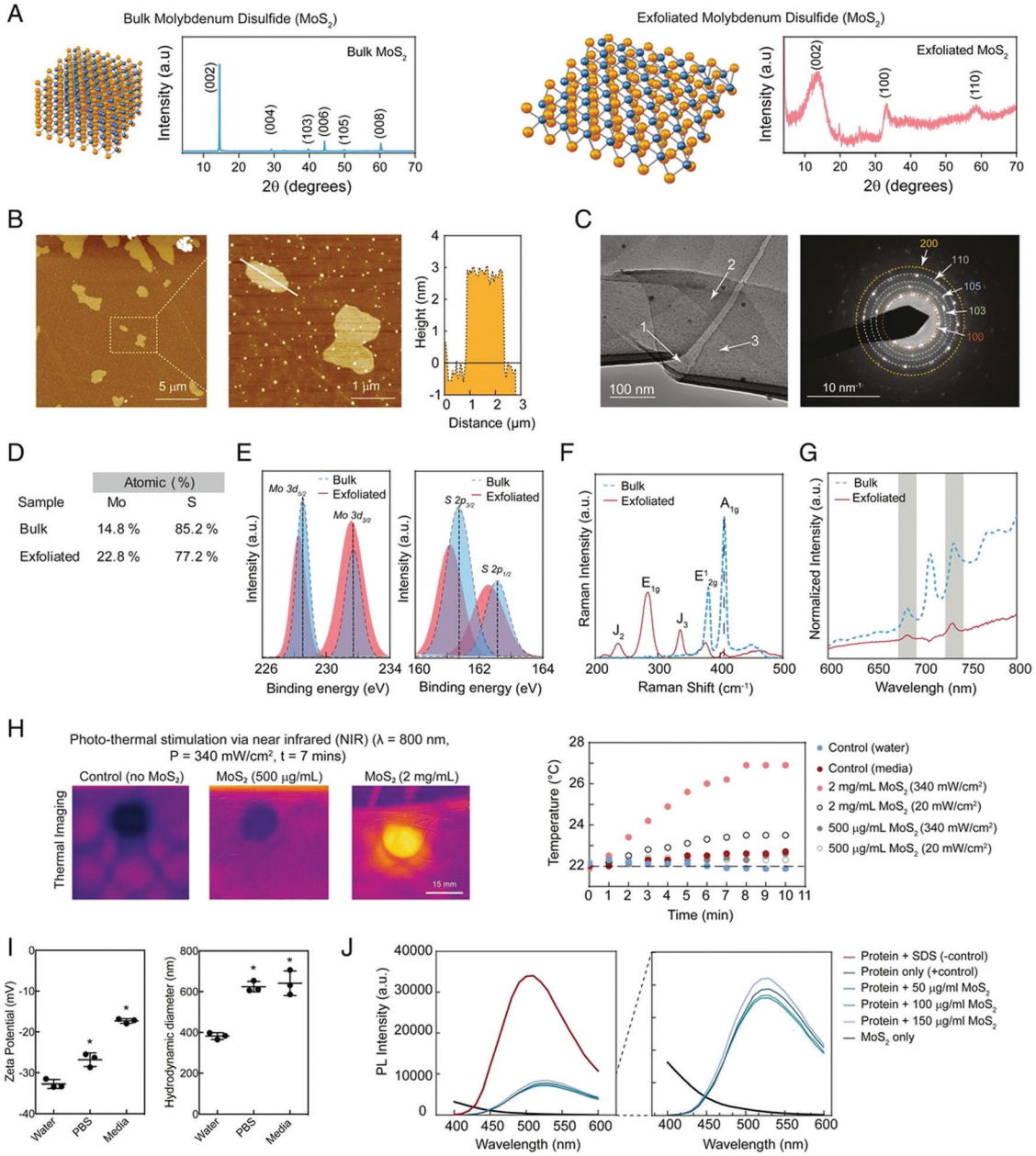

Fig. 3 Physicochemical characterization of exfoliated 2D MoS2 nanosheets. (A) X-ray diffractogram of bulk and exfoliated MoS2, (B) atomic force microscopy (AFM) for confirming the 2D shape, (C) transmission electron microscopy (TEM) images of ultrathin MoS_2 sheets along with electron diffraction pattern, (D) atomic composition of bulk and exfoliated MoS2 determined *via* elemental analysis, (E) X-ray photoelectron spectroscopy (XPS) analysis, (F) Raman spectroscopy, (G) photoluminescent measurements, (H) response to near infra-red (NIR) light was determined using an infra-red (IR) camera and change in temperature over time, (I) zeta potential and hydrodynamic size of exfoliated MoS_2 in water, phosphate buffer saline (PBS), and media, and (J) 8-anilino-1-naphthalenesulfonic acid (ANS) assay shows protein structures are intact in the presence of exfoliated MoS_2.[128]

The study highlighted the effect of protein adsorption on 2D MoS_2 on cellular adhesion and internalization because of the formation of protein corona on MoS_2 nanosheets (Fig. 3).

Cellular adhesion is a crucial parameter in the area of wound healing and tissue repair as in the case of tissue engineering, the adhesion of cells to the external scaffolds directly affects the tissue repair process. In this regard, Seung *et al.* studied the self-healing and adhesion property of monolayer MoS_2 and silicon oxide.[129] The concept could have utility in designing novel MoS_2-based scaffolds for tissue engineering applications. Further, the work carried out by Manish *et al.* sheds light upon the wetting characteristics by modulating the super-hydrophobic states of 2D MoS_2 that could be achieved by controlling the atomic-level defects in MoS_2 nanostructures.[130] The modulation in atomic defects of MoS_2 nanostructures is suggested to have direct implications on the cell adhesion characteristics that could be leveraged for tissue engineering and biomedical applications. However, Anna *et al.* evaluated

the applicability of surfactant-free liquid-phase exfoliated 2D MoS_2 as a platform for the treatment and detection of cancer.[131] In order to further enhance the selectivity and efficiency of this 2D MoS_2-based platform, the system was equipped with antigen–antibody binding modalities. The detection of cancer cells is based on the level of internalization efficacy of cancer cells towards a modified 2D MoS_2-based detection system. Further, assessment of cellular proliferation could be a vital stat to drive this process for advancement.

The surface chemistry of a material plays a crucial role in tissue engineering applications. The type of bonds formed between the material and the cell surface dictates the efficiency of adhesion and in turn, affects cellular behaviour and proliferation. In order to utilize the MoS_2 nanostructures-based scaffolds for tissue engineering applications, the surface functionality and modifications need to be carried out in a proficient manner. This will impart better control over cell adhesion, proliferation and differentiation, which is very essential for an effective tissue regeneration strategy.

3.3. Immunomodulatory properties

The recent surge in MoS_2 nanostructures-based research has led to the utility of MoS_2 in numerous fields ranging from cutting-edge electronic devices to biomedical applications. However, in order to evaluate the impact of MoS_2 on human health, the necessity to understand the interaction of MoS_2 with a biological system is crucial. When a tissue confronts adverse conditions (tissue damage, injury, autoimmune response, or infections), the defense system of our body tends to protect or minimize the impairment caused through a complex biological response known as inflammation.[132] The complete process of inflammation involves a series of well-organized and dynamic responses comprising both cellular and vascular events with specific humoral secretions.[133] Inflammatory response mainly includes cells of the immune systems and inflammatory modulators.[134] The innate immune response of a body is governed by cytokines which include pro-inflammatory cytokines such as interleukin (IL)-1β (IL-1β), IL-6, IL-8, and tumour necrosis factor-α (TNF-α), and anti-inflammatory cytokines such as IL-10.[135]

Accompanied by its widespread applicability, the immunomodulatory response of MoS_2 has also gained considerable attention owing to its utility in biomedical applications. In this regard, Moore *et al.* studied the inflammatory responses of different sized MoS_2 flakes on various cell lines (monocyte, THP-1; inhalation, A549; ingestion, AGS), which were selected to represent different means of exposure.[136] This work demonstrated the size-dependent response of macrophages with the smallest sized MoS_2 flake exercising maximum cytokine upregulation. This size dependency of the macrophage response could be associated with the increased concentration of endotoxin on the surface of the nanomaterial. As the size decreases, the surface-to-volume ratio increases, thereby providing more surfaces for exposure. However, Gu *et al.* studied the underlying mechanism of MoS_2-mediated immune response in detail.[137] The work included both molecular dynamics simulation and flow cytometric experimentations to investigate the molecular mechanism of cytokines production by MoS_2 and PEG-functionalized MoS_2. Moreover, Han *et al.* reported the fabrication of nanoconjugates of MoS_2 nanosheets functionalized with cytosine–phosphate–guanine (CpG) and PEG.[138] The fabricated nanoconjugate was reported to have augmented the cellular uptake of pristine MoS_2 and improved the production of pro-inflammatory cytokines leading to an efficient immune response. The study presented the capability to modulate immunotherapy-based cancer treatment. To further investigate the immunomodulating properties of MoS_2, Jiang *et al.* fabricated MoS_2–CuO heteronanocomposites loaded with bovine serum albumin and imiquimod (R837), an immunoadjuvant.[139] In this study, it was demonstrated that MoS_2–CuO nanocomposites were able to generate hydroxyl free radicals when exposed to overproduced hydrogen peroxide in tumours. The study also reported the ability of the designed nanocomposites for modulating immunotherapy-based cancer treatment. For a successful regeneration of damaged tissue, inflammation, repair and remodeling are the three main phases. The efficiency and time taken in crossing each phase are very crucial and decide the fate of the tissue regeneration process. While designing a scaffold for tissue engineering, assessment of the immunological process is very important. In terms of exploring MoS_2-based scaffolds for tissue engineering, major emphasis could be given to designing immune-compatible scaffolds by incorporating external agents such as fibrinogen and interleukins.

Zhan and co-workers further investigated the immunostimulatory property of 2D MoS_2. Their study reported the role of few-layered MoS_2 nanosheets in enhancing dendritic cells (DC) maturation, migration and T cell elicitation.[140] In this work, the migration ability of DCs was examined upon the introduction of MoS_2 nanosheets (MSNs). It was also demonstrated that the exposure of MSNs increases the migration distance and velocity of DCs compared to non-treated controls. The work presented a detailed study on the important parameters of dendritic cells such as maturation, migration and T cell activation backed with statistical analysis. Activation and proliferation of CD^{4+} and CD^{8+} T cells were observed at *in vivo* levels, implicating immunomodulating effects of MoS_2 nanosheets (Fig. 4). Moreover, Baimanov *et al.* studied the immunological responses of MoS_2 nanosheets–protein corona complexes.[141] They provided an insight into the pro-inflammatory effect of native MoS_2 nanosheets and their complex with blood proteins and highlighted the contribution of blood proteins corona towards the enhancement of inflammatory responses of MoS_2 nanosheets. All these studies revealed the immunomodulatory effect of MoS_2. Assessment of the immunological response of MoS_2 will provide important insights for the safety evaluation of MoS_2 based nanostructures. This will further ensure the fabrication of rational MoS_2-based designs to be used for tissue engineering applications.

4. MoS_2-based nanostructures in tissue engineering

Tissue engineering is a dynamic field that deals with the regeneration of tissues/organs that are damaged or incapable of

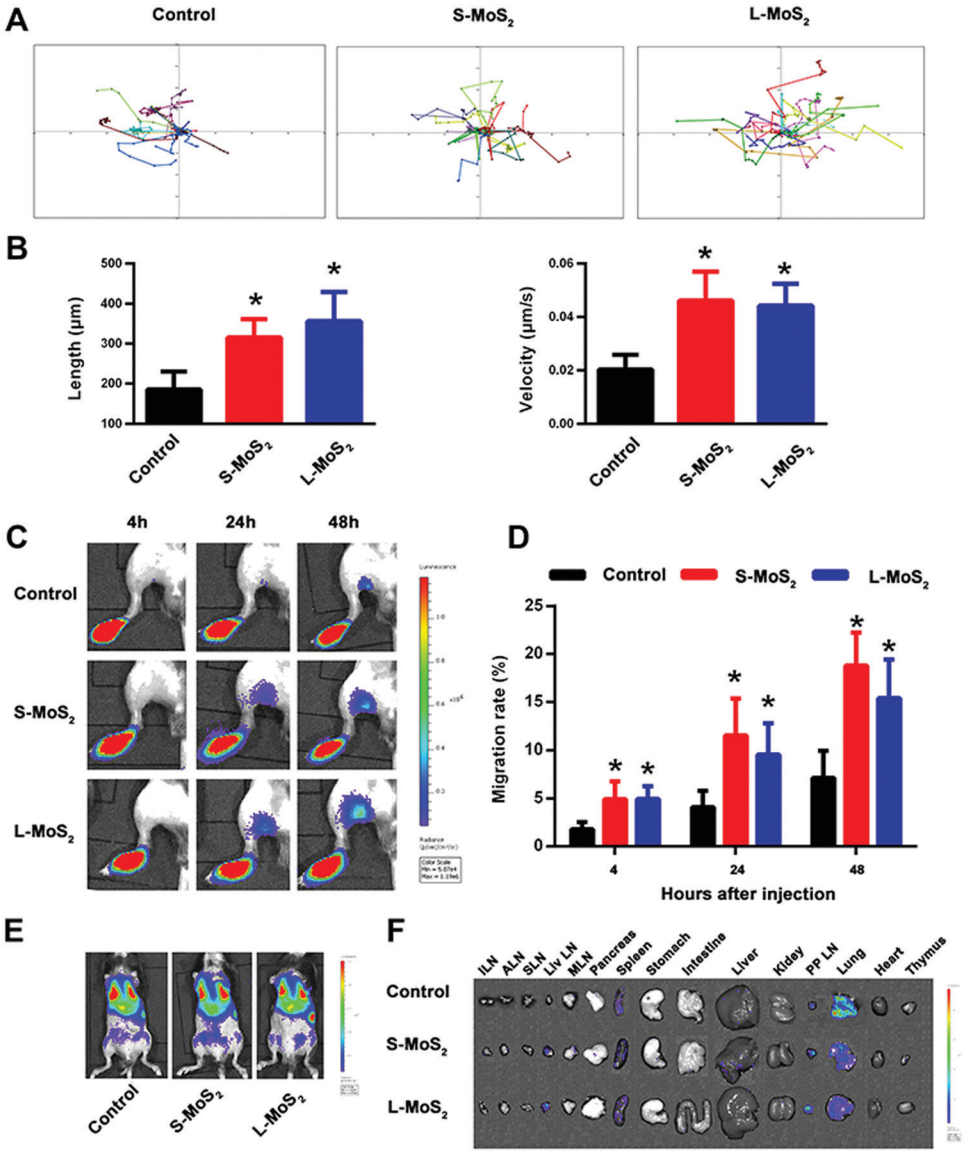

Fig. 4 MSNs improved the *ex vivo* movement and *in vivo* homing ability of DCs. Notes: (A) the *ex vivo* movement of DCs, (B) statistical data of the length and velocity of DC movement. (C) The *in vivo* homing of tissue-resident DCs, (D) statistical data of the homing percentage. N = five for each group. (E) Imaging of the overall distribution of intravenously injected $Fluc^+$ DCs at 2 h. (F) The tissue accumulation of circulating DCs at 48 h after injection.[140]

self-revival. In order to engineer a tissue construct, cells are usually seeded on scaffolds/biomaterials that imitate the extracellular matrix (ECM) and tissue microenvironment to aid in tissue development. Biodegradable polymers (synthetic and natural), nanocomposites, and porous scaffolds have been under constant investigation to be used for tissue engineering applications.[142] Generally, the scaffolds designed using polymer composites/nanocomposites and biomaterials for tissue regeneration must possess high porosity that is helpful in inducing cell migration, nutrient transportation and tissue growth.[143] However, in certain cases, the mechanical stability (in case of bone tissue engineering),[144] and conducting nature (in case of neural and cardiac tissue engineering)[145] of the designed scaffolds could also play a crucial role.

In this regard, MoS_2-based nanostructures are being explored owing to their remarkable properties of high surface area/mass ratio, decent electrical conductivity, exceptional optical properties, and suitable biocompatibility.[113] The application of femtosecond (fs) laser pulses to micropattern MoS_2/acrylamide electrospun nanofibers was studied by Paula *et al.*[146] The work reported the impact on the topography of composite nanofiber under the influence of laser pulse energy and scanning speed. The application of fs laser resulted in the formation of micropores while preserving the nature of the composite nanofibers. The proposed nanofibers could be utilized for their applicability in the field of tissue engineering due to the additional advantage of photoluminescence and enhanced mechanical strength upon strengthening with MoS_2. Further, Chen *et al.* proposed CVD-grown monolayer MoS_2 nanosheets to use as bioabsorbable electronics-based biosensors.[147] The cytotoxicity and biocompatibility studies of

the as-synthesized MoS_2 nanosheets provided a set of parameters that could be vital in understanding the effectiveness of the synthesized nanosheets for biological systems. The study emphasized the enhancement of the dissolution rate of the monolayer MoS_2 in PBS solution upon reduction of its grain size and intensification of intrinsic defects. This feature could be very important in terms of controlling the lifetime of the designed material and its usefulness as a scaffold for tissue engineering applications and wearable implants.

To further implicate the applicability of 2D MoS_2 in tissue engineering, biosensors, and electrochemical electrodes, Sim *et al.* fabricated silk fibroin exfoliated MoS_2 nanosheets with a high yield.[148] The study presented a detailed investigation of silk fibroin-based MoS_2 dispersions as a function of centrifugation speed, time taken for sonication, and initial concentrations of silk powder and solvent. In order to design effective MoS_2 based scaffolds for tissue engineering applications, the yield and uniformity of MoS_2 nanostructures are very important. Careful assessment and controlling of these parameters will result in the fabrication of scaffolds with enhanced immunomodulation and tissue regeneration ability.

MoS_2 has also been mixed with other low dimensional nanomaterials to further improve the scaffold properties and impart a synergistic effect in terms of mechanical strength that

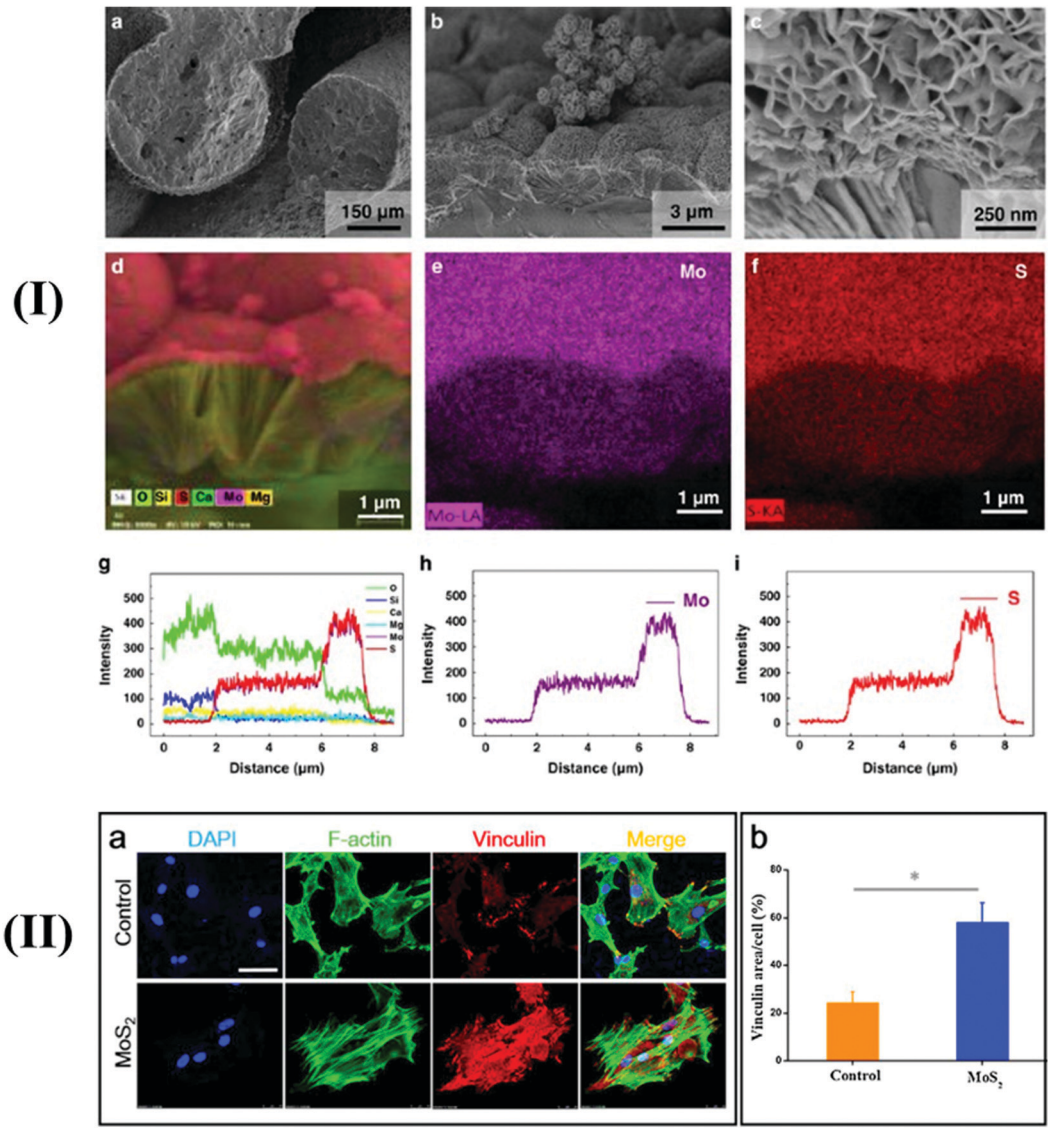

Fig. 5 (I) Fracture morphologies of 0.2 MoS_2-modified akermanite (MS-AKT) scaffolds at different magnifications (a–c), energy-dispersive spectrometer (EDS) elemental mapping of the cross-section of MoS_2–AKT interface: all elements (d), element Mo (e), element S (f); EDS line scanning profiles of all elements (g), element Mo (h) and element S (i) from the interior to the strut surface of the scaffolds, which exhibited a step profile, confirming the elemental interpermeation between MoS_2 and AKT.[149] (II) Immunostaining of the focal adhesion protein vinculin. (a) Vinculin (red fluorescence) of MSCs grown on the flat substrate and the nanostructured MoS_2. Scale bar: 25 m. The images are merged images of F-actin (green fluorescence), vinculin (red fluorescence) and DAPI (blue fluorescence). (b) Percentage of the vinculin expressed area against the cell spreading area. Reproduced with permission from.[151] Copyright 2018 Elsevier.

is advantageous for tissue engineering applications. In a study by Feng *et al.*, 0 D nanodiamond particles and MoS_2 nanosheets were uniformly dispersed into poly (3-hydroxybutyrate-*co*-3-hydroxyvalerate) (PHBV) scaffolds using selective laser sintering. However, the synergistic effect of graphene oxide with MoS_2 was studied by Wan *et al.* High mechanical strength was recorded for these reinforced and synthesized scaffolds and a detailed mechanism concerning their enhanced tensile and compressive strength was also reported with enhanced electrical conductivity and mechanical property. These studies have provided a new approach for designing scaffolds for various organ-specific tissue engineering applications. The proceeding section will further discuss a few specific tissue engineering aspects in detail.

4.1. Bone tissue engineering

Ailments related to the bone have global predominance since they can be occurred due to multiple causes, which include cancer, injuries, and accidents. Since its inception in the early 90s, bone tissue engineering has always been explored to fabricate inventive novel biological materials that could aid in bone regeneration and enhance the repairing process. Wang *et al.* explored the synergistic effect of MoS_2 in both tissue engineering and tumor therapy by fabricating a bifunctional scaffold of MoS_2 nanosheets grown on 3D-printed bioceramic scaffolds of akermanite (AKT) ($Ca_2MgSi_2O_7$) *in situ*. It was also demonstrated that, upon irradiation, the temperature of the designed scaffold (MS-AKT) rapidly increased, which in turn decreased the viability of osteosarcoma cells and breast cancer cells, thereby inhibiting the growth of tumours *in vivo*. Further, MS-AKT scaffolds supported the cell adhesion, proliferation, osteogenic differentiation of bone mesenchymal stem cells, and encouraged bone regeneration *in vivo*. The fabrication method was a merger of 3D printing technology and the hydrothermal method.[149] The ability of the designed scaffold to generate bone was also tested at *in vitro* and *in vivo* levels (Fig. 5(I)). Moreover, Wang *et al.* reported a novel scaffold of 2D MoS_2–PLGA with 3D printed bioactive borosilicate glass as a platform for the synergistic treatment of bone repair and tumor therapy.[150] The prepared scaffolds could stimulate proliferation and differentiation of rat bone mesenchymal stem cells and promoted bone repair for calvarial defects in the rat. With high photothermal efficiency, the designed scaffold has promising futuristic applications for bone cancer-related defects. All these studies assessed the ability of MoS_2 nanostructure-based scaffolds to support and promote osteogenic differentiation and angiogenesis. Further, a hydrothermal method was employed by Zhang *et al.* to fabricate MoS_2 for tissue engineering applications.[151] In this work, the influence of MoS_2 on the focal adhesion (FA) was detected using the immunofluorescent staining for detecting vinculin (adaptor protein forming FA). Apart from the focal adhesion formation, upregulation of osteogenic genes and cell proliferation was added advantage of the synthesized MoS_2 nanostructures (Fig. 5(II)).

The bone-forming ability of akermanite-based scaffolds has been reported by Huang *et al.* with beta-tricalcium phosphate (beta-TCP) as a control.[152] Further, Liu *et al.* reported the effect of akermanite-based scaffolds on the proliferation, adhesion, and osteogenic differentiation of human adipose-derived stem cells.[153] The application of MoS_2 in the akermanite scaffold not only improved bone regeneration but also showed applicability in tumor reduction. This makes it a promising material for

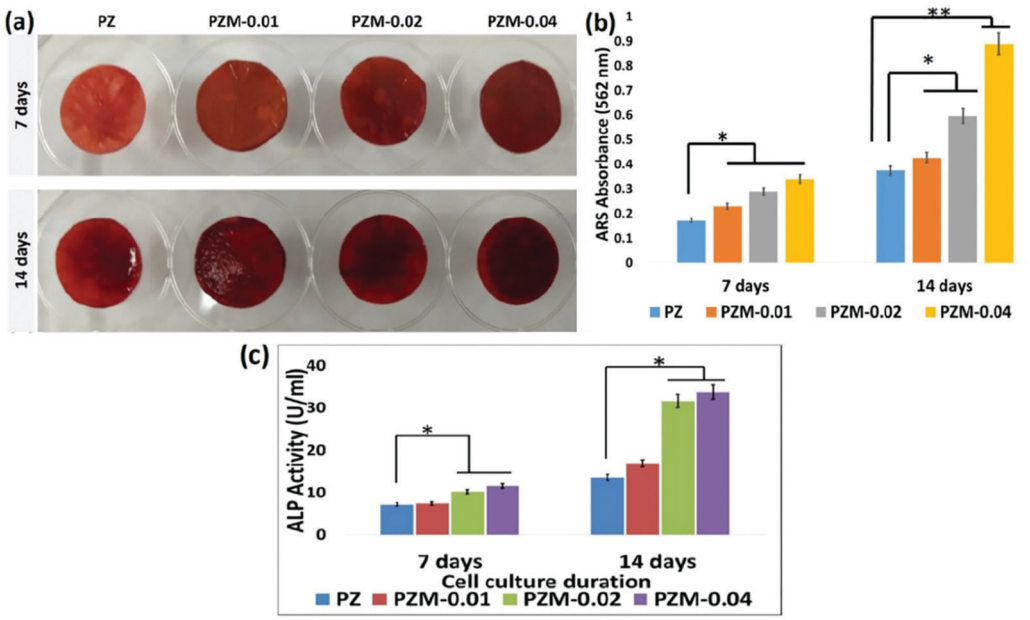

Fig. 6 ARS staining and alkaline phosphate (ALP) test results. (a) The digital images, (b) absorbance data, and (c) ALP activity. For ARS, the respective scaffolds were stained at (7 and 14) days. The ALP activity was also evaluated on (7 and 14 days). Reproduced with permission from ref. 155. Copyright 2020 Elsevier.

tumor-induced bone defects. Furthermore, Wu *et al.* combined the electrospinning technique with doping to fabricate polyacrylonitrile/MoS_2 nanofibrous scaffolds.[154] The designed scaffolds promoted cell proliferation and activity and offered excellent biocompatibility and osteogenic differentiation. The ability of MoS_2 as an excellent reinforcement for bone tissue engineering was further explored by Awasthi *et al.* who fabricated polycaprolactone/zein (PZ) composite nanofibers supplemented with albumin induced exfoliated MoS_2 nanosheets (PZM).[155] The MoS_2-reinforced scaffold offered improved wettability and mechanical properties compared to the pristine polycaprolactone/zein composite nanofibers. Improved calcium–phosphate deposition upon assessment with simulated body fluid (SBF) biomineralization and Alizarin Red S (ARS) test were added advantages associated with MoS_2-reinforced composite nanofibers (Fig. 6).

In order to tackle the *in situ* bacterial infection and promote osteointegration of orthopaedic implants, Yuan *et al.* fabricated MoS_2/polydopamine/RGD peptide coated titanium implants. The work highlighted the capability of the modified titanium implants to kill bacteria with an efficiency of almost 92% upon NIR radiation exposure without causing damage to the normal tissue. The work could be applicable for reoccurring infections after surgery and could have significant potential for bone tissue engineering, as antibacterial and upregulation of genes responsible for osteogenesis. The capability of 2D MoS_2-reinforced hydroxyapatite (HAP) scaffolds to provide osteogenic differentiation, proliferation, and bone regeneration at *in vitro* and *in vivo* levels was investigated by Yadav *et al.*[156] The cells incubated with the designed scaffolds presented higher cell adhesion and proliferation along with enhanced alkaline phosphatase activity (ALP). The obtained results were also supported with increased levels of osteogenic markers and bone morphogenetic protein-2.

Moreover, for a successful bone tissue engineering outcome, enhancement in the osteogenic process is very important as it gives a clear indication of repair of bone deformations and

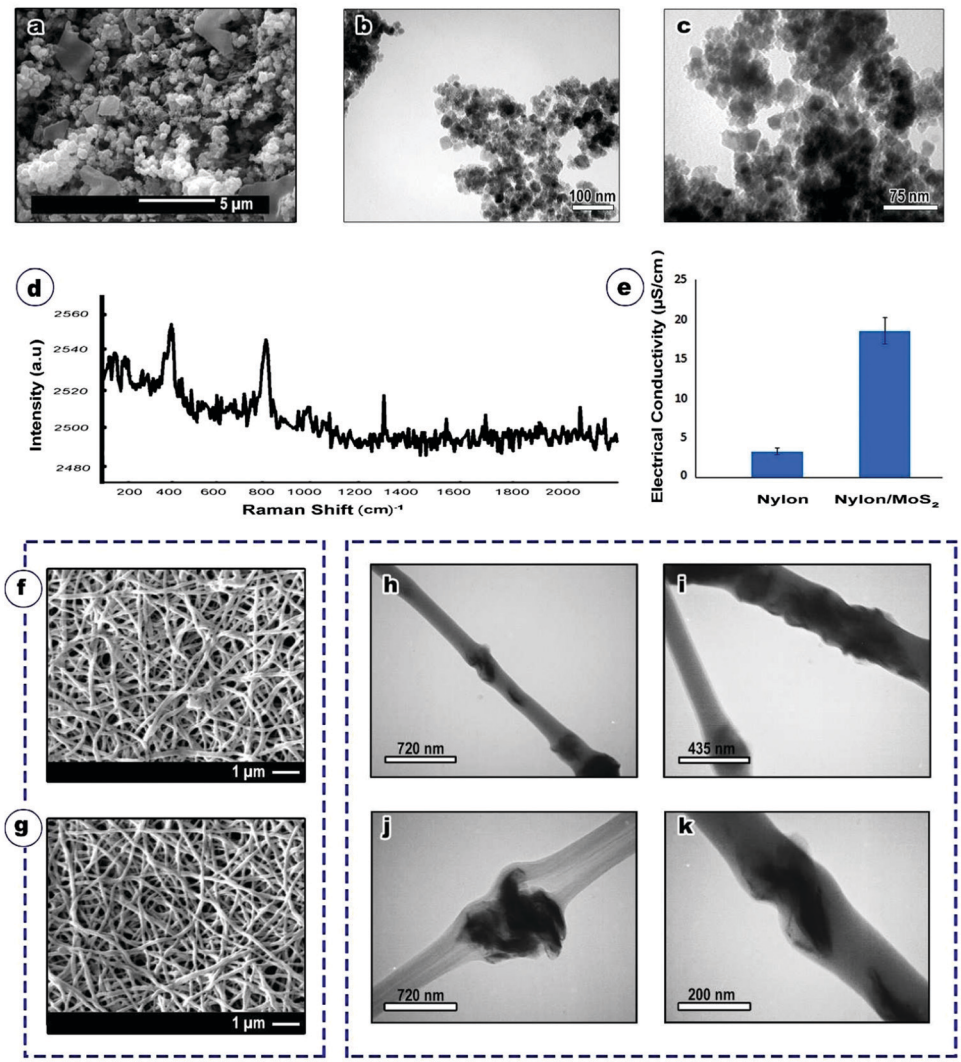

Fig. 7 (a) Scanning electron microscopy (SEM) image of MoS_2 nanosheets, (b and c) TEM images of MoS_2 nanosheets, (d) Raman spectroscopy MoS_2, (e) electrical conductivity of nylon and nylon/MoS2 scaffolds, (f and g) SEM micrograph of nylon and nylon/MoS_2 nanofibers, (g–k) TEM micrograph of nylon/MoS_2 nanofibers. Reproduced with permission from ref. 157. Copyright 2019 Wiley.

injuries. The regeneration of bone without the aid of external growth factors further provides a promising outcome for a potent scaffold for tissue engineering applications. Apart from high porosity and pore interconnectivity, load-bearing efficiency is also very crucial while designing scaffolds. Further research could be implemented to study the load-bearing capacity of MoS_2 based scaffolds.

4.2. Cardiac tissue engineering

The field of cardiac tissue engineering deals with the repair and regeneration of cardiac tissues, muscles and cells. Close coordination between the cardiac cells and the support system (scaffold) is required for effective cardiac tissue regeneration. The application of MoS_2 nanosheets in cardiac tissue engineering was studied by Nazari *et al.* The study reported the fabrication of electrospun nanofibers of MoS_2 nanosheets incorporated nylon 6.[157] In this work, the fabricated MoS_2 NPs were mostly in the shape of nanosheets with a size of approximately 400 nm with the presence of some sheet-like nanostructures with a size >2 μm. In addition, the mean diameter of nylon and nylon/MoS_2 nanofibers was found to be approximately 182 and 161 nm, respectively (Fig. 7). The synthesized nanofibers offered high mechanical properties and enhanced electrical conductivity with improved cell proliferation and attachment. The study emphasized the ability of MoS_2 to upregulate cardiac functional genes and induction of cardiogenic differentiation and maturation of mouse embryonic cardiac cells (mECCs). The electrical signaling response of MoS_2-based scaffolds needs to be investigated in detail as this could open gates for the intense utilization of MoS_2-based scaffolds for nerve and cardiac tissue engineering. Further, the application of MoS_2 to enhance the mechanical, electrical, thermal and structural properties of chitosan was studied by Feng *et al.*[158] The reinforcement effect and well dispersion state of MoS_2 with chitosan were credited for the enhancement in the properties of pristine chitosan films. This work could be utilized to develop MoS_2–chitosan scaffolds for

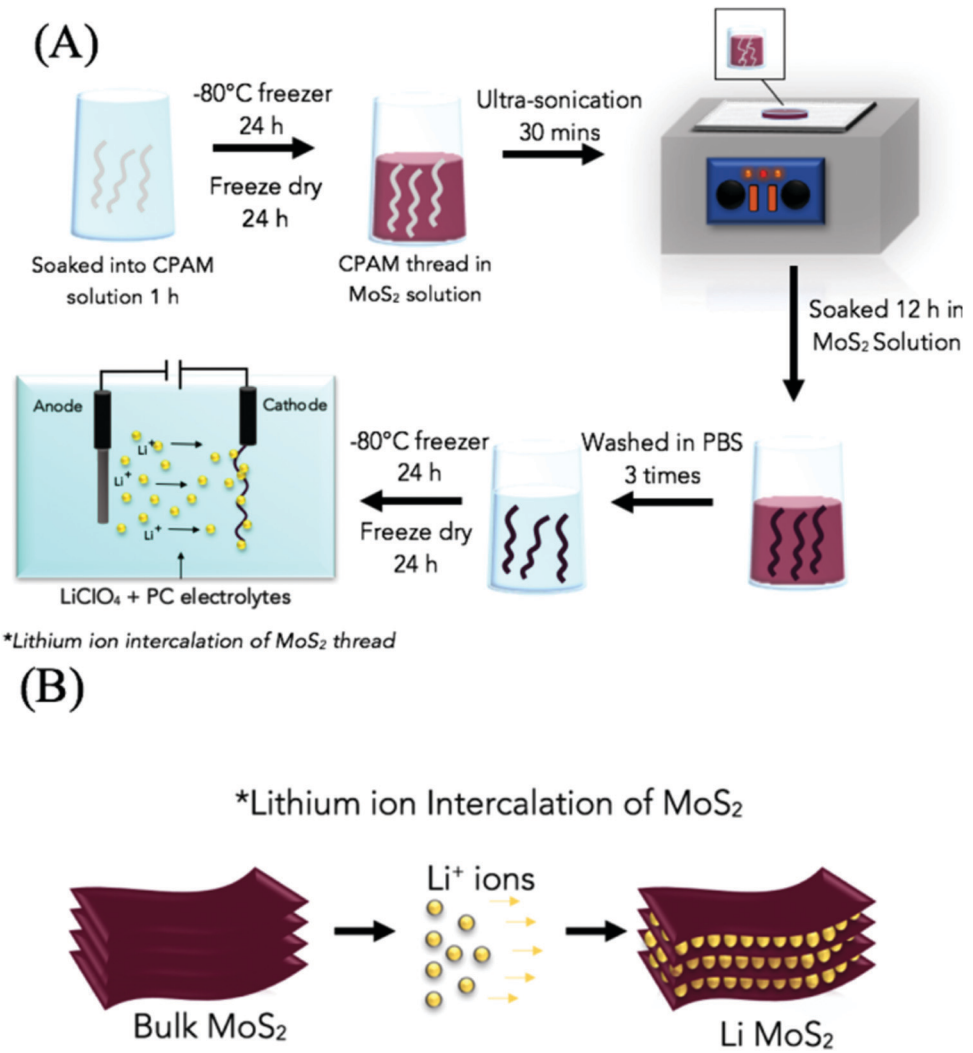

Fig. 8 (A) Schematic diagram illustrating the workflow of pre-treating the thread with cationic polyacrylamide (CPAM) and preparing lithium-intercalated MoS_2 nanoflake coated thread. (B) Depiction of lithium-ion intercalation of MoS_2-thread to render the thread conductive, Reproduced with permission from ref. 161. Copyright 2019 American Chemical Society.

providing necessary electrical stimulus that can be explored for cardiac tissue engineering applications. The regeneration of functional cardiac tissues with adequate response will have a significant impact in eradicating many ailments related to cardiovascular tissue damage. The properties of cardiogenic differentiation, cell adhesion, and proliferation should be the key parameters to be targeted while designing scaffolds for cardiac tissue beginning.

4.3. Neural tissue engineering

The cases of nerve injuries are on the rise and can be a result of accidents, trauma, ailment, and congenital defects. However, nerves with a gap smaller than 1 cm could be restored through the surgical process but large nerve injuries are difficult to fix.[159,160] In order to meet this demand, designing biocompatible artificial cylindrical constructs imitating the structural and functional property of nerves has been intensively explored. In this regard, Taheri *et al.* developed lithium intercalated MoS_2-coated cotton thread as a potent candidate for nerve tissue-engineering applications[161] (Fig. 8). Apart from testing the biocompatibility and cytotoxicity of the designed scaffolds for multiple cell lines, the conductivity and permeability of the scaffolds were also evaluated. The work could impart an opportunity to fabricate biomimetic fibrillary construction of the ECM. In another study, Wang *et al.* investigated the application of PVDF–MoS_2 scaffolds for promoting neural stem cell (NSC) differentiation with high efficiency and without including external growth factors.[162] In this work, the immunofluorescent staining method was executed with precise neural markers, such as neuronal associated class III beta-tubulin protein (Tuj1) and glial fibrillary acidic protein (GFAP), to account for the degree of differentiation of NSCs into neural cell types. The study showed a positive effect that the nanostructured MTFs exhibit significantly positive effects on NSC proliferation and attachment with negligible cytotoxicity.

Good electrical conductivity and large surface area are tagged as added advantages associated with the designed scaffolds that help ion cell adhesion and proliferation. The

Table 2 MoS_2-based scaffolds for tissue engineering applications

S. No	Nature of MoS_2	Composition	Scaffold type	Processing method	Cell line	Targeted tissue	Features	Ref.
1.	Quantum dots	Polyamide	Nanofibers scaffold	Electrospinning		General	Threshold energy of nanofibrous membrane reduced from 3.5 to 1.8 nJ, uniform distribution of MoS_2 in the membrane, micropatterning of pillars	146
2.	Nanosheets	Silk fibroin	Nanosheets	Freeze-dried		General	Significant output for scale up, thickness of 3–6 nm, high aqueous stability	148
3.	Nanosheets	Akermanite	Scaffold	3D-printing technology and hydrothermal method	Saos-2 cells, MDA-MB-231 cells	Bone tissue engineering	Supports cell attachment, proliferation and osteogenic differentiation of rBMSCs, induced bone regeneration at *in vivo* level	149
4.	Nanosheets	Bioactive borosilicate glass	Scaffold	3D-printing technology	MNNG/HOS cells	Bone tissue engineering	Retention up to 60 days, tumour therapy, stimulate differentiation of rBMSCs, upregulate osteogenic genes expression	150
5.	Nanoflakes	Fluorine doped tin oxide coated glass	Scaffold	Hydrothermal method	rBMSCs	Bone tissue engineering	Formation of focal adhesion between cells and substrate, promoted osteogenesis	151
6.	Nanofibers	Polyacrylonitrile	Composite nanofibers scaffold	Electrospinning technology	rBMSCs	Bone tissue engineering	Promote rBMSCs growth, proliferation and activity	154
7.	Nanosheets	Polycaprolactone, zein	Composite nanofibers scaffold	Albumin-induced exfoliation	MC3T3-E1	Bone tissue engineering	Enhanced cell attachment, proliferation and differentiation	155
8.	Nanosheets	Hydroxyapatite	Nanocomposite scaffold	Hydrothermal method	MG-63 cells	Bone tissue engineering	*In vitro* and *in vivo* osteogenic differentiation, proliferation, rapid osteogenesis	156
9.	Nanoflakes	Nylon	Nanofibers scaffold	Electrospinning technology	mECCs	Cardiac tissue engineering	Maturation and upregulation of cardiac functional genes, elongated morphology	157
10.	Nanoflakes	Chitosan	Composite scaffolds	Acidic exfoliation		General	Enhanced mechanical and thermal properties	158
11.	Nanoflakes	Cotton thread	Thread scaffolds	Exfoliation and Electrochemical method	NG108-15, PC 12	Nerve tissue engineering	Electrical conductivity of 9.4 × 101 S m^{-1}, cell proliferation over a period of 3 days	161
	Nanosheets	Polyvinylidene fluoride	Nanofibrous scaffold	Hydrothermal method and electrospinning technology	NSC	Nerve tissue engineering	Promote cell differentiation of NSC and neural maturation,	162

field of MoS_2 based neural tissue engineering is still under exploration and has a lot of potential. In this area, inspecting the simulation-based electrical signalling response of designed scaffolds will certainly have an edge in further developing improved scaffolds with remarkable properties. A detailed summary of the applications of MoS_2-based nanostructures for different organ-specific tissue engineering is provided in Table 2.

5. Conclusions and future prospective

MoS_2-based nanostructures signify as one of the most promising and attractive materials for numerous applications ranging from the industrial segment to the biomedical field. The unique set of physicochemical properties associated with MoS_2 nanostructures makes it an exceptional candidate for its widespread utility. The review discusses the different structural arrangements (2D, 1D, 0D) in which MoS_2 could be perceived. The review also addressed the structural-based alterations in the properties of different MoS_2-based nanostructural morphologies. To further investigate the compatibility of MoS_2 with biological systems, comprehensive wisdom of their cellular interaction is very essential. Thus, the effect of nanostructured MoS_2 on cellular toxicity, biocompatibility, proliferation, adhesion, and immunomodulation is thoroughly reviewed. This will render an approximation of the level of MoS_2 that could be utilized for their applicability with biological systems. The review further presents a comprehensive overview of the exploitation of nanostructured MoS_2 in tissue engineering applications with emphasis on bone, cardiac and neural tissue engineering. Further, the tissue-specific features of the fabricated MoS_2-based scaffolds are thoroughly reviewed and analyzed to implicate their practicality in regenerating large organs as well.

Although, considerable progress is still underway in terms of the applicability of nanostructured MoS_2-based scaffolds for tissue engineering applications, in-depth knowledge of the cellular interaction of MoS_2 is deficient. Different forms and sizes of any material will give an altered response when exposed to a living system, which in turn will affect the anticipated application of any material. This unlocks new opportunities, which need to be explored to design effective MoS_2-based scaffolds for tissue engineering applications. In addition, novel strategies to synthesize and functionalize uniform MoS_2 nanostructures with substantial control over their size and properties will further aid in their widespread utility. However, in order to utilize MoS_2-based scaffolds for large tissue regeneration such as skin, further refinement in fabricating process is required. To design such scaffolds, imitating ECM could not be the sole criteria but repair and improvement of diseased tissue ECM is a vital criterion to be handled for effectual tissue regeneration. To tackle this hurdle, additive manufacturing techniques could be explored for effectual MoS_2-based scaffold production. An interdisciplinary approach with collaborative effort is necessary to see the clinical translation of nanostructured MoS_2-based scaffolds for tissue engineering applications.

Data availability

The data that support the tables within this article and other findings of this study are available from the corresponding author upon reasonable request.

Author contributions

Anuj Kumar: conceptualization, methodology, investigation, writing – original draft, writing – review & editing, supervision, funding acquisition. Ankur Sood: methodology, investigation, software, writing – original draft. Sung Soo Han: writing – review & editing, supervision, funding acquisition.

Conflicts of interest

The authors declare that they have no known competing financial interests or personal relationships that could have appeared to influence the work reported in this paper.

Acknowledgements

This work was supported by the National Research Foundation of Korea (NRF) funded by the Ministry of Education, Science and Technology, grant numbers ''2021R1I1A3059994, 2020K-1A3A1A19088873, 2020R1A2C1012586, and 2020R1A6A1AA03-044512''. Authors of this work thank the authors whose research or review articles have been cited in this review article.

References

1 N. Baig, I. Kammakakam and W. Falath, *Mater. Adv.*, 2021, **2**, 1821–1871.
2 V. Yadav, S. Roy, P. Singh, Z. Khan and A. Jaiswal, *Small*, 2019, **15**, 1803706.
3 K. Zhao, W. Zhu, S. Liu, X. Wei, G. Ye, Y. Su and Z. He, *Nanoscale Adv.*, 2020, **2**, 536–562.
4 H. Park, D. S. Oh, K. J. Lee, D. Y. Jung, S. Lee, S. Yoo and S.-Y. Choi, *ACS Appl. Mater. Interfaces*, 2020, **12**, 4749–4754.
5 D. Zhou, L. Zhao and B. Li, *J. Energy Chem.*, 2021, **62**, 27–42.
6 W. Yin, L. Yan, J. Yu, G. Tian, L. Zhou, X. Zheng, X. Zhang, Y. Yong, J. Li, Z. Gu and Y. Zhao, *ACS Nano*, 2014, **8**, 6922–6933.
7 A. Bolotsky, D. Butler, C. Dong, K. Gerace, N. R. Glavin, C. Muratore, J. A. Robinson and A. Ebrahimi, *ACS Nano*, 2019, **13**, 9781–9810.
8 A. McCreary, O. Kazakova, D. Jariwala and Z. Y. Al Balushi, *2D Mater.*, 2020, **8**, 013001.
9 A. S. Sethulekshmi, J. S. Jayan, S. Appukuttan and K. Joseph, *Phys. E*, 2021, **132**, 114716.
10 X. Yin, C. S. Tang, Y. Zheng, J. Gao, J. Wu, H. Zhang, M. Chhowalla, W. Chen and A. T. S. Wee, *Chem. Soc. Rev.*, 2021, **50**, 10087–10115.

11 T. Cao, G. Wang, W. Han, H. Ye, C. Zhu, J. Shi, Q. Niu, P. Tan, E. Wang, B. Liu and J. Feng, *Nat. Commun.*, 2012, **3**, 887.
12 F. Bussolotti, H. Kawai, Z. E. Ooi, V. Chellappan, D. Thian, A. L. C. Pang and K. E. J. Goh, *Nano Futures*, 2018, **2**, 032001.
13 S. Manzeli, D. Ovchinnikov, D. Pasquier, O. V. Yazyev and A. Kis, *Nat. Rev. Mater.*, 2017, **2**, 17033.
14 G. Zhang, H. Liu, J. Qu and J. Li, *Energy Environ. Sci.*, 2016, **9**, 1190–1209.
15 J. Ryou, Y.-S. Kim, S. Kc and K. Cho, *Sci. Rep.*, 2016, **6**, 29184.
16 M. Timpel, G. Ligorio, A. Ghiami, L. Gavioli, E. Cavaliere, A. Chiappini, F. Rossi, L. Pasquali, F. Gärisch, E. J. W. List-Kratochvil, P. Nozar, A. Quaranta, R. Verucchi and M. V. Nardi, *npj 2D Mater. Appl.*, 2021, **5**, 64.
17 C. Liu, Y. Bai, Y. Zhao, H. Yao and H. Pang, *Energy Storage Mater.*, 2020, **33**, 470–502.
18 Z. Yang, L. Zhu, C. Lv, R. Zhang, H. Wang, J. Wang and Q. Zhang, *Mater. Chem. Front.*, 2021, **5**, 5880–5896.
19 W. Li, G. Liu, J. Li, Y. Wang, L. Ricardez-Sandoval, Y. Zhang and Z. Zhang, *Appl. Surf. Sci.*, 2019, **498**, 143869.
20 S. Niu, J. Cai and G. Wang, *Nano Res.*, 2021, **14**, 1985–2002.
21 W. Wang, G. N. Panin, X. Fu, L. Zhang, P. Ilanchezhiyan, V. O. Pelenovich, D. Fu and T. W. Kang, *Sci. Rep.*, 2016, **6**, 31224.
22 F. Wu, S. Si, P. Cao, W. Wei, X. Zhao, T. Shi, X. Zhang, J. Ma, R. Cao, L. Liao, T.-Y. Tseng and Q. Liu, *Adv. Electron. Mater.*, 2019, **5**, 1800747.
23 N. Pallikkarathodi Mani, M. Ganiga and J. Cyriac, *Analyst*, 2018, **143**, 1691–1698.
24 L. Lan, D. Chen, Y. Yao, X. Peng, J. Wu, Y. Li, J. Ping and Y. Ying, *ACS Appl. Mater. Interfaces*, 2018, **10**, 42009–42017.
25 S. Das, Y. Wang, Y. Dai, S. Li and Z. Sun, *Light: Sci. Appl.*, 2021, **10**, 27.
26 C. Fu, L. Tan, X. Ren, Q. Wu, H. Shao, J. Ren, Y. Zhao and X. Meng, *Chem. Commun.*, 2018, **54**, 13989–13992.
27 T. Liu and Z. Liu, *Adv. Healthcare Mater.*, 2018, **7**, 1701158.
28 K. Zhang, Y. Zhuang, W. Zhang, Y. Guo and X. Liu, *Drug Delivery*, 2020, **27**, 909–916.
29 R. Deng, H. Yi, F. Fan, L. Fu, Y. Zeng, Y. Wang, Y. Li, Y. Liu, S. Ji and Y. Su, *RSC Adv.*, 2016, **6**, 77083–77092.
30 M. Zhang, K. Wang, S. Zeng, Y. Xu, W. Nie, P. Chen and Y. Zhou, *Chem. Eng. J.*, 2021, **411**, 128517.
31 S. Roy, A. Mondal, V. Yadav, A. Sarkar, R. Banerjee, P. Sanpui and A. Jaiswal, *ACS Appl. Bio Mater.*, 2019, **2**, 2738–2755.
32 J. Li, J. Zheng, Y. Yu, Z. Su, L. Zhang and X. Chen, *Nanotechnology*, 2020, **31**, 125101.
33 S. Barua, H. S. Dutta, S. Gogoi, R. Devi and R. Khan, *ACS Appl. Nano Mater.*, 2018, **1**, 2–25.
34 Z. Hu, R. Xu, S. Yu, J. Li and Z. Yang, *Analyst*, 2020, **145**, 7864–7869.
35 C. Song, C. Yang, F. Wang, D. Ding, Y. Gao, W. Guo, M. Yan, S. Liu and C. Guo, *J. Mater. Chem. B*, 2017, **5**, 9015–9024.
36 H. Jiang, Y. Du, L. Chen, M. Qian, Y. Yang, T. Huo, X. Yan, T. Ye, B. Han, Y. Wang and R. Huang, *Int. J. Pharm.*, 2020, **586**, 119606.
37 E. A. Makris, A. H. Gomoll, K. N. Malizos, J. C. Hu and K. A. Athanasiou, *Nat. Rev. Rheumatol.*, 2015, **11**, 21–34.
38 Y. Zheng, X. Hong, J. Wang, L. Feng, T. Fan, R. Guo and H. Zhang, *Adv. Healthcare Mater.*, 2021, **10**, 2001743.
39 E. P. Nguyen, C. de Carvalho Castro Silva and A. Merkoçi, *Nanoscale*, 2020, **12**, 19043–19067.
40 S. A. Han, R. Bhatia and S.-W. Kim, *Nano Convergence*, 2015, **2**, 17.
41 M. Chhowalla, H. S. Shin, G. Eda, L.-J. Li, K. P. Loh and H. Zhang, *Nat. Chem.*, 2013, **5**, 263–275.
42 K. S. Novoselov, D. Jiang, F. Schedin, T. J. Booth, V. V. Khotkevich, S. V. Morozov and A. K. Geim, *Proc. Natl. Acad. Sci. U. S. A.*, 2005, **102**, 10451–10453.
43 W. Zhao, J. Pan, Y. Fang, X. Che, D. Wang, K. Bu and F. Huang, *Chem. – Eur. J.*, 2018, **24**, 15942–15954.
44 C. Ataca, H. Şahin and S. Ciraci, *J. Phys. Chem. C*, 2012, **116**, 8983–8999.
45 W. Choi, N. Choudhary, G. H. Han, J. Park, D. Akinwande and Y. H. Lee, *Mater. Today*, 2017, **20**, 116–130.
46 X. Duan, C. Wang, A. Pan, R. Yu and X. Duan, *Chem. Soc. Rev.*, 2015, **44**, 8859–8876.
47 E. Canadell, A. LeBeuze, M. A. El Khalifa, R. Chevrel and M. H. Whangbo, *J. Am. Chem. Soc.*, 1989, **111**, 3778–3782.
48 H. Xu, J. Zhu, Q. Ma, J. Ma, H. Bai, L. Chen and S. Mu, *Micromachines*, 2021, **12**, 240.
49 A. Chaves, J. G. Azadani, H. Alsalman, D. R. da Costa, R. Frisenda, A. J. Chaves, S. H. Song, Y. D. Kim, D. He, J. Zhou, A. Castellanos-Gomez, F. M. Peeters, Z. Liu, C. L. Hinkle, S.-H. Oh, P. D. Ye, S. J. Koester, Y. H. Lee, P. Avouris, X. Wang and T. Low, *npj 2D Mater. Appl.*, 2020, **4**, 29.
50 H. D. Ha, D. J. Han, J. S. Choi, M. Park and T. S. Seo, *Small*, 2014, **10**, 3858–3862.
51 K. Kalantar-zadeh and J. Z. Ou, *ACS Sens.*, 2016, **1**, 5–16.
52 A. Castellanos-Gomez, M. Poot, G. A. Steele, H. S. J. van der Zant, N. Agraït and G. Rubio-Bollinger, *Adv. Mater.*, 2012, **24**, 772–775.
53 S. Bertolazzi, J. Brivio and A. Kis, *ACS Nano*, 2011, **5**, 9703–9709.
54 M. Liu, K. Hisama, Y. Zheng, M. Maruyama, S. Seo, A. Anisimov, T. Inoue, E. I. Kauppinen, S. Okada, S. Chiashi, R. Xiang and S. Maruyama, *ACS Nano*, 2021, **15**, 8418–8426.
55 P. Chithaiah, S. Ghosh, A. Idelevich, L. Rovinsky, T. Livneh and A. Zak, *ACS Nano*, 2020, **14**, 3004–3016.
56 R. Tenne, L. Margulis, M. Genut and G. Hodes, *Nature*, 1992, **360**, 444–446.
57 M. Remskar, A. Mrzel, M. Virsek, M. Godec, M. Krause, A. Kolitsch, A. Singh and A. Seabaugh, *Nanoscale Res. Lett.*, 2010, **6**, 26.
58 G. Seifert, H. Terrones, M. Terrones, G. Jungnickel and T. Frauenheim, *Phys. Rev. Lett.*, 2000, **85**, 146–149.
59 M. Damnjanović, T. Vuković and I. Milošević, *Isr. J. Chem.*, 2017, **57**, 450–460.

60 H.-U. Kim, H. Kim, C. Ahn, A. Kulkarni, M. Jeon, G. Y. Yeom, M.-H. Lee and T. Kim, *RSC Adv.*, 2015, **5**, 10134–10138.
61 T. Liu, C. Wang, X. Gu, H. Gong, L. Cheng, X. Shi, L. Feng, B. Sun and Z. Liu, *Adv. Mater.*, 2014, **26**, 3433–3440.
62 M. Remškar, M. Viršek and A. Mrzel, *Appl. Phys. Lett.*, 2009, **95**, 133122.
63 D. Bera, L. Qian, T.-K. Tseng and P. H. Holloway, *Materials*, 2010, **3**, 2260–2345.
64 X. Tong, X. Zhan, D. Rawach, Z. Chen, G. Zhang and S. Sun, *Prog. Nat. Sci.: Mater. Int.*, 2020, **30**, 787–795.
65 B. Li, L. Jiang, X. Li, P. Ran, P. Zuo, A. Wang, L. Qu, Y. Zhao, Z. Cheng and Y. Lu, *Sci. Rep.*, 2017, **7**, 11182.
66 Y. Hao, W. Su, L. Hou, X. Cui, S. Wang, P. Zhan, Y. Zou, L. Fan and J. Zheng, *Sci. China Mater.*, 2020, **63**, 1046–1053.
67 J. Benson, M. Li, S. Wang, P. Wang and P. Papakonstantinou, *ACS Appl. Mater. Interfaces*, 2015, **7**, 14113–14122.
68 D. Vikraman, K. Akbar, S. Hussain, G. Yoo, J.-Y. Jang, S.-H. Chun, J. Jung and H. J. Park, *Nano Energy*, 2017, **35**, 101–114.
69 H. Lin, C. Wang, J. Wu, Z. Xu, Y. Huang and C. Zhang, *New J. Chem.*, 2015, **39**, 8492–8497.
70 H. Nan, Z. Wang, W. Wang, Z. Liang, Y. Lu, Q. Chen, D. He, P. Tan, F. Miao, X. Wang, J. Wang and Z. Ni, *ACS Nano*, 2014, **8**, 5738–5745.
71 C. Sweet, A. Pramanik, S. Jones and P. C. Ray, *ACS Omega*, 2017, **2**, 1826–1835.
72 W. Gu, Y. Yan, C. Zhang, C. Ding and Y. Xian, *ACS Appl. Mater. Interfaces*, 2016, **8**, 11272–11279.
73 L. Liu, H. Jiang, J. Dong, W. Zhang, G. Dang, M. Yang, Y. Li, H. Chen, H. Ji and L. Dong, *Colloids Surf., B*, 2020, **185**, 110590.
74 M. Yi and C. Zhang, *RSC Adv.*, 2018, **8**, 9564–9573.
75 Y. Takahashi, Y. Nakayasu, K. Iwase, H. Kobayashi and I. Honma, *Dalton Trans.*, 2020, **49**, 9377–9384.
76 G. Deokar, D. Vignaud, R. Arenal, P. Louette and J. F. Colomer, *Nanotechnology*, 2016, **27**, 075604.
77 S. Thangudu, M. T. Lee and S. Rtimi, *Catalysts*, 2020, **10**, 1009.
78 N. J. A. Cordeiro, C. Gaspar, M. J. d. Oliveira, D. Nunes, P. Barquinha, L. Pereira, E. Fortunato, R. Martins, E. Laureto and S. A. Lourenço, *Appl. Sci.*, 2021, **11**, 1234.
79 X. Li, A. Tang, J. Li, L. Guan, G. Dong and F. Teng, *Nanoscale Res. Lett.*, 2016, **11**, 171.
80 H. Zhou, R. Zhang, S. Song, C. Xiao, G. Gao and S. Ding, *ACS Appl. Energy Mater.*, 2018, **1**, 5112–5118.
81 C. Perumal Veeramalai, F. Li, H. Xu, T. W. Kim and T. Guo, *RSC Adv.*, 2015, **5**, 57666–57670.
82 Z. Tu, G. Li, X. Ni, L. Meng, S. Bai, X. Chen, J. Lou and Y. Qin, *Appl. Phys. Lett.*, 2016, **109**, 223101.
83 R. Wei, H. Zhang, X. He, Z. Hu, X. Tian, Q. Xiao, Z. Chen and J. Qiu, *Opt. Mater. Express*, 2015, **5**, 1807–1814.
84 S. S. Sinha, L. Yadgarov, S. B. Aliev, Y. Feldman, I. Pinkas, P. Chithaiah, S. Ghosh, A. Idelevich, A. Zak and R. Tenne, *J. Phys. Chem. C*, 2021, **125**, 6324–6340.
85 Y. Zhong, D. Liu, L.-T. Wang, H.-g. Zhu and G. Hong, *J. Colloid Interface Sci.*, 2020, **561**, 593–600.
86 J. Chen, S.-L. Li, Q. Xu and K. Tanaka, *Chem. Commun.*, 2002, 1722–1723.
87 X. Zhang, X. Li, J. Liang, Y. Zhu and Y. Qian, *Small*, 2016, **12**, 2484–2491.
88 M. Baby and K. Rajeev Kumar, *Mater. Sci. Technol.*, 2019, **35**, 1416–1427.
89 G. Pradhan, P. P. Dey, A. Khare and A. K. Sharma, *J. Appl. Phys.*, 2021, **129**, 025112.
90 M. Shrivastava, R. Kumari, M. R. Parra, P. Pandey, H. Siddiqui and F. Z. Haque, *Opt. Mater.*, 2017, **73**, 763–771.
91 J. Ali, G. U. Siddiqui, K. H. Choi, Y. Jang and K. Lee, *J. Lumin.*, 2016, **169**, 342–347.
92 S. J. Park, S. W. Pak, D. Qiu, J. H. Kang, D. Y. Song and E. K. Kim, *J. Lumin.*, 2017, **183**, 62–67.
93 Y. Zhong and T. Yi, *J. Mater. Chem. B*, 2019, **7**, 2549–2556.
94 S.-J. An, D. Y. Park, C. Lee, S. Bang, D. A. Nguyen, S. H. Kim, H. Y. Kim, H. J. Jeong and M. S. Jeong, *Appl. Surf. Sci.*, 2020, **511**, 145507.
95 H. Yang, A. Giri, S. Moon, S. Shin, J.-M. Myoung and U. Jeong, *Chem. Mater.*, 2017, **29**, 5772–5776.
96 D. Kong, H. Wang, J. J. Cha, M. Pasta, K. J. Koski, J. Yao and Y. Cui, *Nano Lett.*, 2013, **13**, 1341–1347.
97 A. Hasani, Q. V. Le, M. Tekalgne, M.-J. Choi, T. H. Lee, H. W. Jang and S. Y. Kim, *NPG Asia Mater.*, 2019, **11**, 47.
98 Y.-H. Lee, X.-Q. Zhang, W. Zhang, M.-T. Chang, C.-T. Lin, K.-D. Chang, Y.-C. Yu, J. T.-W. Wang, C.-S. Chang, L.-J. Li and T.-W. Lin, *Adv. Mater.*, 2012, **24**, 2320–2325.
99 J. Jung, J. Lee, Y. Kim, H. Bark and C. Lee, *J. Phys. D: Appl. Phys.*, 2019, **52**, 18LT01.
100 S. Barua and S. Mitragotri, *Nano Today*, 2014, **9**, 223–243.
101 P. Shah, T. N. Narayanan, C.-Z. Li and S. Alwarappan, *Nanotechnology*, 2015, **26**, 315102.
102 J. Jian, H. Chang and T. Xu, *Materials*, 2019, **12**, 198.
103 F. Yin, T. Anderson, N. Panwar, K. Zhang, S. C. Tjin, B. K. Ng, H. S. Yoon, J. Qu and K. T. Yong, *Nanotheranostics*, 2018, **2**, 371–386.
104 Z. Sobańska, L. Zapór, M. Szparaga and M. Stępnik, *Int. J. Occup. Med. Environ. Health*, 2020, **33**, 1–19.
105 A. Murali, G. Lokhande, K. A. Deo, A. Brokesh and A. K. Gaharwar, *Mater. Today*, 2021, **50**, 276–302.
106 E. L. K. Chng, Z. Sofer and M. Pumera, *Nanoscale*, 2014, **6**, 14412–14418.
107 R. Wu, X. Ou, R. Tian, J. Zhang, H. Jin, M. Dong, J. Li and L. Liu, *Nanoscale*, 2018, **10**, 20162–20170.
108 X. Yang, J. Li, T. Liang, C. Ma, Y. Zhang, H. Chen, N. Hanagata, H. Su and M. Xu, *Nanoscale*, 2014, **6**, 10126–10133.
109 M. H. Shin, S. M. Baek, A. V. Polyakov, I. P. Semenova, R. Z. Valiev, W. B. Hwang, S. K. Hahn and H. S. Kim, *Sci. Rep.*, 2018, **8**, 9907.
110 J. Fan, Y. Li, H. N. Nguyen, Y. Yao and D. F. Rodrigues, *Environ. Sci.: Nano*, 2015, **2**, 370–379.

111 C. Wang, J. Li, X. Liu, Z. Cui, D.-F. Chen, Z. Li, Y. Liang, S. Zhu and S. Wu, *Biomater. Sci.*, 2020, **8**, 4216–4224.
112 X. Yang, J. Li, T. Liang, C. Ma, Y. Zhang, H. Chen, N. Hanagata, H. Su and M. Xu, *Nanoscale*, 2014, **6**, 10126–10133.
113 W. Z. Teo, E. L. Chng, Z. Sofer and M. Pumera, *Chem. – Eur. J.*, 2014, **20**, 9627–9632.
114 X. Wang, N. D. Mansukhani, L. M. Guiney, Z. Ji, C. H. Chang, M. Wang, Y.-P. Liao, T.-B. Song, B. Sun, R. Li, T. Xia, M. C. Hersam and A. E. Nel, *Small*, 2015, **11**, 5079–5087.
115 B. Domi, K. Bhorkar, C. Rumbo, L. Sygellou, S. N. Yannopoulos, R. Quesada and J. A. Tamayo-Ramos, *Nanotechnology*, 2020, **31**, 445101.
116 Z. Wang, A. von dem Bussche, Y. Qiu, T. M. Valentin, K. Gion, A. B. Kane and R. H. Hurt, *Environ. Sci. Technol.*, 2016, **50**, 7208–7217.
117 L. Dong, S. Lin, L. Yang, J. Zhang, C. Yang, D. Yang and H. Lu, *Chem. Commun.*, 2014, **50**, 15936–15939.
118 J. Hao, G. Song, T. Liu, X. Yi, K. Yang, L. Cheng and Z. Liu, *Adv. Sci.*, 2017, **4**, 1600160.
119 K. Bazaka, I. Levchenko, J. W. M. Lim, O. Baranov, C. Corbella, S. Xu and M. Keidar, *J. Phys. D: Appl. Phys.*, 2019, **52**, 183001.
120 R. Kurapati, L. Muzi, A. P. R. de Garibay, J. Russier, D. Voiry, I. A. Vacchi, M. Chhowalla and A. Bianco, *Adv. Funct. Mater.*, 2017, **27**, 1605176.
121 D. Voiry, A. Goswami, R. Kappera, C. e Silva Cde, D. Kaplan, T. Fujita, M. Chen, T. Asefa and M. Chhowalla, *Nat. Chem.*, 2015, **7**, 45–49.
122 Y. L. Huang, Y. Chen, W. Zhang, S. Y. Quek, C.-H. Chen, L.-J. Li, W.-T. Hsu, W.-H. Chang, Y. J. Zheng, W. Chen and A. T. S. Wee, *Nat. Commun.*, 2015, **6**, 6298.
123 J. Shi, J. Li, Y. Wang, J. Cheng and C. Y. Zhang, *J. Mater. Chem. B*, 2020, **8**, 5793–5807.
124 A. Abareshi, M. Arshadi Pirlar and M. Houshiar, *Mater. Res. Express*, 2019, **6**, 105050.
125 Y. Zhang, W. Jiang, D. Feng, C. Wang, Y. Xu, Y. Shan, J. Wang, Z. Yin, H. Deng, X. Mi and N. Dai, *Nanomaterials*, 2021, **11**, 545.
126 X. Zhu, X. Ji, N. Kong, Y. Chen, M. Mahmoudi, X. Xu, L. Ding, W. Tao, T. Cai, Y. Li, T. Gan, A. Barrett, Z. Bharwani, H. Chen and O. C. Farokhzad, *ACS Nano*, 2018, **12**, 2922–2938.
127 K. Jin, L. Xie, Y. Tian and D. Liu, *J. Phys. Chem. C*, 2016, **120**, 11204–11209.
128 J. K. Carrow, K. A. Singh, M. K. Jaiswal, A. Ramirez, G. Lokhande, A. T. Yeh, T. R. Sarkar, I. Singh and A. K. Gaharwar, *Proc. Natl. Acad. Sci. U. S. A.*, 2020, **117**, 13329–13338.
129 S. R. Na, Y. Kim, C. Lee, K. M. Liechti and J. W. Suk, *Sci. Rep.*, 2017, **7**, 14740.
130 M. K. Jaiswal, K. A. Singh, G. Lokhande and A. K. Gaharwar, *Chem. Commun.*, 2019, **55**, 8772–8775.
131 A. Kálosi, M. Labudová, A. Annušová, M. Benkovičová, M. Bodík, J. Kollár, M. Kotlár, P. Kasak, M. Jergel, S. Pastoreková, P. Siffalovic and E. Majkova, *Biomater. Sci.*, 2020, **8**, 1973–1980.
132 V. Chiurchiù, A. Leuti and M. Maccarrone, *Front. Immunol.*, 2018, **9**, 38.
133 L. A. Abdulkhaleq, M. A. Assi, R. Abdullah, M. Zamri-Saad, Y. H. Taufiq-Yap and M. N. M. Hezmee, *Vet. World*, 2018, **11**, 627–635.
134 S. M. Lucas, N. J. Rothwell and R. M. Gibson, *Br. J. Pharmacol.*, 2006, **147**(suppl 1), S232–S240.
135 C. A. Howell, S. R. Sandeman, G. J. Phillips, A. W. Lloyd, J. G. Davies, S. V. Mikhalovsky, S. R. Tennison, A. P. Rawlinson, O. P. Kozynchenko, H. L. H. Owen, J. D. S. Gaylor, J. J. Rouse and J. M. Courtney, *Biomaterials*, 2006, **27**, 5286–5291.
136 C. Moore, D. Movia, R. J. Smith, D. Hanlon, F. Lebre, E. C. Lavelle, H. J. Byrne, J. N. Coleman, Y. Volkov and J. McIntyre, *2D Mater.*, 2017, **4**, 025065.
137 Z. Gu, S. H. Chen, Z. Ding, W. Song, W. Wei, S. Liu, G. Ma and R. Zhou, *Nanoscale*, 2019, **11**, 22293–22304.
138 Q. Han, X. Wang, X. Jia, S. Cai, W. Liang, Y. Qin, R. Yang and C. Wang, *Nanoscale*, 2017, **9**, 5927–5934.
139 F. Jiang, B. Ding, S. Liang, Y. Zhao, Z. Cheng, B. Xing, P. Ma and J. Lin, *Biomaterials*, 2021, **268**, 120545.
140 L. Deng, X. Pan, Y. Zhang, S. Sun, L. Lv, L. Gao, P. Ma, H. Ai, Q. Zhou, X. Wang and L. Zhan, *Int. J. Nanomed.*, 2020, **15**, 2971–2986.
141 D. Baimanov, J. Wu, R. Chu, R. Cai, B. Wang, M. Cao, Y. Tao, J. Liu, M. Guo, J. Wang, X. Yuan, C. Ji, Y. Zhao, W. Feng, L. Wang and C. Chen, *ACS Nano*, 2020, **14**, 5529–5542.
142 G. Lalwani, A. M. Henslee, B. Farshid, P. Parmar, L. Lin, Y. X. Qin, F. K. Kasper, A. G. Mikos and B. Sitharaman, *Acta Biomater.*, 2013, **9**, 8365–8373.
143 A.-V. Do, B. Khorsand, S. M. Geary and A. K. Salem, *Adv. Healthcare Mater.*, 2015, **4**, 1742–1762.
144 M. Xu, H. Li, D. Zhai, J. Chang, S. Chen and C. Wu, *J. Mater. Chem. B*, 2015, **3**, 3799–3809.
145 A. Burnstine-Townley, Y. Eshel and N. Amdursky, *Adv. Funct. Mater.*, 2020, **30**, 1901369.
146 K. T. Paula, L. A. Mercante, R. Schneider, D. S. Correa and C. R. Mendonca, *Photonics*, 2019, **6**, 3.
147 X. Chen, Y. J. Park, M. Kang, S.-K. Kang, J. Koo, S. M. Shinde, J. Shin, S. Jeon, G. Park, Y. Yan, M. R. MacEwan, W. Z. Ray, K.-M. Lee, J. A. Rogers and J.-H. Ahn, *Nat. Commun.*, 2018, **9**, 1690.
148 H. Sim, J. Lee, B. Park, S. J. Kim, S. Kang, W. Ryu and S. C. Jun, *Nano Res.*, 2016, **9**, 1709–1722.
149 X. Wang, T. Li, H. Ma, D. Zhai, C. Jiang, J. Chang, J. Wang and C. Wu, *NPG Asia Mater.*, 2017, **9**, e376.
150 H. Wang, X. Zeng, L. Pang, H. Wang, B. Lin, Z. Deng, E. L. X. Qi, N. Miao, D. Wang, P. Huang, H. Hu and J. Li, *Chem. Eng. J.*, 2020, **396**, 125081.
151 X. Zhang, J. Nie, X. Yang, Z. Liu, W. Guo, J. Qiu, S. Wang, X. Yu, Y. Guan, H. Liu and L. Li, *Appl. Mater. Today*, 2018, **10**, 164–172.
152 Y. Huang, X. Jin, X. Zhang, H. Sun, J. Tu, T. Tang, J. Chang and K. Dai, *Biomaterials*, 2009, **30**, 5041–5048.

153 Q. Liu, L. Cen, S. Yin, L. Chen, G. Liu, J. Chang and L. Cui, *Biomaterials*, 2008, **29**, 4792–4799.
154 S. Wu, J. Wang, L. Jin, Y. Li and Z. Wang, *ACS Appl. Nano Mater.*, 2018, **1**, 337–343.
155 G. P. Awasthi, V. K. Kaliannagounder, B. Maharjan, J. Y. Lee, C. H. Park and C. S. Kim, *Mater. Sci. Eng., C*, 2020, **116**, 111162.
156 U. Yadav, H. Mishra, V. Singh, S. Kashyap, A. Srivastava, S. Yadav and P. S. Saxena, *ACS Biomater. Sci. Eng.*, 2019, **5**, 4511–4521.
157 H. Nazari, A. Heirani-Tabasi, M. S. Alavijeh, Z. S. Jeshvaghani, E. Esmaeili, S. Hosseinzadeh, F. Mohabatpour, B. Taheri, S. H. A. Tafti and M. Soleimani, *ChemistrySelect*, 2019, **4**, 11557–11563.
158 X. Feng, X. Wang, W. Xing, K. Zhou, L. Song and Y. Hu, *Compos. Sci. Technol.*, 2014, **93**, 76–82.
159 H. Fujimaki, K. Uchida, G. Inoue, M. Miyagi, N. Nemoto, T. Saku, Y. Isobe, K. Inage, O. Matsushita, S. Yagishita, J. Sato, S. Takano, Y. Sakuma, S. Ohtori, K. Takahashi and M. Takaso, *J. Biomed. Mater. Res., Part A*, 2017, **105**, 8–14.
160 M. Nune, U. M. Krishnan and S. Sethuraman, *Mater. Sci. Eng., C*, 2016, **62**, 329–337.
161 N. Sadeghi Taheri, Y. Wang, K. Berean, P. Chan and K. Kalantar Zadeh, *ACS Appl. Nano Mater.*, 2019, **2**, 2044–2053.
162 S. Wang, J. Qiu, W. Guo, X. Yu, J. Nie, J. Zhang, X. Zhang, Z. Liu, X. Mou, L. Li and H. Liu, *Adv. Biosyst.*, 2017, **1**, e1600042.

